

# Saxagliptin and Tadalafil Differentially Alter Cyclic Guanosine Monophosphate (cGMP) Signaling and Left Ventricular Function in Aortic-Banded Mini-Swine

Jessica A. Hiemstra, BS; Dong I. Lee, PhD; Khalid Chakir, PhD; Manuel Gutiérrez-Aguilar, PhD; Kurt D. Marshall, MS; Pamela J. Zgoda, BS; Noelany Cruz Rivera, BS; Daniel G. Dozier, BS; Brian S. Ferguson, PhD; Denise M. Heublein, CLT; John C. Burnett, MD; Carolin Scherf, BS; Jan R. Ivey, BS; Gianmaria Minervini, MD; Kerry S. McDonald, PhD; Christopher P. Baines, PhD; Maike Krenz, MD; Timothy L. Domeier, PhD; Craig A. Emter, PhD

**Background**—Cyclic guanosine monophosphate-protein kinase G-phosphodiesterase 5 signaling may be disturbed in heart failure (HF) with preserved ejection fraction, contributing to cardiac remodeling and dysfunction. The purpose of this study was to manipulate cyclic guanosine monophosphate signaling using the dipeptidyl-peptidase 4 inhibitor saxagliptin and phosphodiesterase 5 inhibitor tadalafil. We hypothesized that preservation of cyclic guanosine monophosphate cGMP signaling would attenuate pathological cardiac remodeling and improve left ventricular (LV) function.

**Methods and Results**—We assessed LV hypertrophy and function at the organ and cellular level in aortic-banded pigs. Concentric hypertrophy was equal in all groups, but LV collagen deposition was increased in only HF animals. Prevention of fibrotic remodeling by saxagliptin and tadalafil was correlated with neuropeptide Y plasma levels. Saxagliptin better preserved integrated LV systolic and diastolic function by maintaining normal LV chamber volumes and contractility (end-systolic pressure-volume relationship, preload recruitable SW) while preventing changes to early/late diastolic longitudinal strain rate. Function was similar to the HF group in tadalafil-treated animals including increased LV contractility, reduced chamber volume, and decreased longitudinal, circumferential, and radial mechanics. Saxagliptin and tadalafil prevented a negative cardiomyocyte shortening-frequency relationship observed in HF animals. Saxagliptin increased phosphodiesterase 5 activity while tadalafil increased cyclic guanosine monophosphate levels; however, neither drug increased downstream PKG activity. Early mitochondrial dysfunction, evident as decreased calcium-retention capacity and Complex II-dependent respiratory control, was present in both HF and tadalafil-treated animals.

**Conclusions**—Both saxagliptin and tadalafil prevented increased LV collagen deposition in a manner related to the attenuation of increased plasma neuropeptide Y levels. Saxagliptin appears superior for treating heart failure with preserved ejection fraction, considering its comprehensive effects on integrated LV systolic and diastolic function. (*J Am Heart Assoc.* 2016;5:e003277 doi: 10.1161/JAHA.116.003277)

**Key Words:** cGMP-PKG-PDE5 • heart failure with preserved ejection fraction • pressure-overload • saxagliptin • tadalafil

Diastolic dysfunction can play an important role in heart failure with preserved ejection fraction (HFpEF), with many factors contributing to the disease including left ventricular (LV) hypertrophy, myocardial fibrosis, impaired calcium reuptake, and energetic abnormalities.<sup>1–4</sup> Cyclic

guanosine monophosphate (cGMP) levels modulate many signaling pathways regulating diastolic function and may inhibit ventricular hypertrophy and stiffness while promoting diastolic relaxation.<sup>5–8</sup> There is growing evidence the cGMP signaling cascade is disturbed in HFpEF patients and could

From the Departments of Biomedical Science (J.A.H., M.G.-A., K.D.M., P.J.Z., N.C.R., D.G.D., B.S.F., J.R.I., C.P.B., C.A.E.), Medical Pharmacology and Physiology (K.S.M., C.P.B., M.K., T.L.D.), and Veterinary Pathobiology (C.S.) and Dalton Cardiovascular Research Center (M.G.-A., K.D.M., C.P.B., M.K.), University of Missouri-Columbia, Columbia, MO; Division of Cardiology, Johns Hopkins Medical Institutions, Baltimore, MD (D.I.L., K.C.); Mayo Clinic, Rochester, MN (D.M.H., J.C.B.); AstraZeneca, Fort Washington, PA (G.M.).

**Correspondence to:** Craig A. Emter, PhD, Department of Biomedical Science, University of Missouri-Columbia, 1600 E Rollins, E117 Veterinary Medicine, Columbia, MO 65211. E-mail: emterc@missouri.edu

Received February 3, 2016; accepted March 3, 2016.

© 2016 The Authors. Published on behalf of the American Heart Association, Inc., by Wiley Blackwell. This is an open access article under the terms of the Creative Commons Attribution-NonCommercial-NoDerivs License, which permits use and distribution in any medium, provided the original work is properly cited, the use is non-commercial and no modifications or adaptations are made.

contribute to diastolic dysfunction.<sup>4,5,9,10</sup> cGMP signaling may be reduced in HF via 3 primary cellular mechanisms: (1) enhanced catabolism through upregulation of specific phosphodiesterases (PDEs); (2) decreased synthesis via impaired natriuretic peptide activation of transmembrane-associated particulate guanylate cyclase receptors; or (3) decreased nitric oxide (NO) stimulation of and/or responsiveness by soluble guanylate cyclase.<sup>5</sup>

One alternative method to potentially impact cGMP signaling is by inhibition of the enzyme dipeptidyl-peptidase 4 (DPP-4). DPP-4 cleaves the N-terminal portion from intact brain natriuretic peptide (BNP)<sub>1–32</sub>, yielding BNP<sub>3–32</sub> that displays significantly reduced myocardial, vascular, and renal effects versus the full peptide.<sup>11–13</sup> DPP-4 has also been shown to reduce NO bioavailability.<sup>14</sup> The positive effects and recent US Food and Drug Administration approval of LCZ696 (a combination angiotensin receptor antagonist and neprilysin inhibitor) on reducing natriuretic peptide cleavage products highlight the therapeutic efficacy of preserving intact BNP in HF.<sup>15</sup> The current study expands on this concept to assess and contrast efficacy of both PDE5 and DPP-4 inhibition to promote cGMP. Therefore, the purpose of this study was to assess the effects of promoting cGMP signaling on LV remodeling and function via 2 mechanisms: (1) stimulating cGMP synthesis with the DPP-4 inhibitor saxagliptin; and (2) reducing cGMP catabolism with the PDE5 inhibitor tadalafil. We performed these experiments in aortic-banded miniature swine exhibiting key clinical characteristics of HFpEF including preserved ejection fraction at rest, diastolic dysfunction, depressed contractile reserve, LV fibrosis, and lung congestion.<sup>16–19</sup> Although we originally hypothesized that preservation of cGMP levels would attenuate pathological remodeling and preserve normal LV function in an experimental setting of HF, our results suggest the myocardial effects of saxagliptin and tadalafil occur independently of increasing downstream protein kinase G (PKG) activity.

## Methods

### Aortic Banding

HF was induced with aortic banding over a period of 24 weeks as previously reported by our laboratory<sup>16–18</sup> with modifications. These modifications included the use of younger pigs (3 months old) and a reduced afterload (50 mm Hg). Intact male Yucatan miniature swine were matched for body mass (10–15 kg) and cardiac function and divided into 4 experimental groups: nonbanded untreated control (CON; n=6), aortic-banded untreated HF (HF; n=7), aortic-banded tadalafil-treated HF (HF-TAD; n=8), and aortic-banded saxagliptin-treated HF (HF-SAX; n=8). The aortic band was placed around the ascending aorta (proximal to the brachiocephalic artery)

and a systolic trans-stenotic gradient of  $\approx 50$  mm Hg was achieved ( $50 \pm 1$ ,  $50 \pm 3$ ,  $48 \pm 2$  for HF, HF-TAD, and HF-SAX, respectively,  $P=NS$ ). The aortic band was set under equivalent hemodynamic conditions for all pigs and characterized by a peripheral vascular mean arterial pressure of  $\approx 90$  mm Hg ( $90 \pm 1$ ,  $92 \pm 1$ ,  $90 \pm 1$  for HF, HF-TAD and HF-SAX, respectively,  $P=NS$ ) under anesthesia using phenylephrine (IV  $1–3 \mu\text{g kg}^{-1} \text{min}^{-1}$ ) at a heart rate of  $\approx 100$  beats/min ( $96 \pm 6$ ,  $112 \pm 6$ , and  $102 \pm 6$  for HF, HF-TAD, and HF-SAX, respectively,  $P=NS$ ). One week after aortic banding, treatment with tadalafil ( $2 \text{ mg} \cdot \text{kg}^{-1}$  twice daily, oral; Eli Lilly, Indianapolis, IN) or saxagliptin ( $10 \text{ mg} \cdot \text{kg}^{-1} \cdot \text{day}^{-1}$ , oral; AstraZeneca Diabetes Alliance, Wilmington, DE) began and continued for 23 weeks. Animals were fed a standard diet averaging 15–20 g/kg once daily and water was provided ad libitum. All animal protocols were in accordance with the “Principles for the Utilization and Care of Vertebrate Animals Used in Testing Research and Training” and approved by the University of Missouri Animal Care and Use Committee.

### Terminal Studies

Animals were initially anesthetized with a telazol ( $5 \text{ mg} \cdot \text{kg}^{-1}$ )/xylazine ( $2.25 \text{ mg} \cdot \text{kg}^{-1}$ ) mix and maintained on propofol ( $6–10 \text{ mg} \cdot \text{kg}^{-1} \cdot \text{min}^{-1}$  with bolus as needed) as previously described.<sup>17</sup> Heparin was given with an initial loading dose of 300 U/kg IV, followed by maintenance of 100 U/kg each hour. A median sternotomy was performed, and pressure-volume (P-V) loops were measured utilizing a calibrated 5F admittance-based ADVantage catheter (Transonic Systems, Inc.; Ithaca, NY) positioned in the LV via a small apical incision. A 14F balloon occlusion catheter was advanced to the inferior vena cava at the level of the apex of the heart via the deep femoral vein.

### In Vivo Cardiovascular Function

P-V experiments were conducted as previously published.<sup>18</sup> Briefly, after the catheters were placed, animals were allowed to stabilize for 10 minutes until a resting, baseline homeostasis was established. P-V loops were recorded under conditions of reducing preload achieved through transient occlusion of the inferior vena cava via inflation of the balloon catheter. Indices of LV function were generated using a minimum of 10 consecutive cardiac cycles with Lab Scribe software (iWorx; Dover, NH) including the following: heart rate, LV end-systolic and diastolic volume, LV end-systolic and diastolic pressure, ejection fraction, and stroke volume. Indices of LV contractility and stiffness including the end-systolic pressure-volume relationship (ESPVR), preload recruitable stroke work (PRSW), and the end-diastolic pressure-volume relationship (EDPVR) were measured using at least 15

consecutive cardiac cycles of constantly reducing preload. A quadratic fit was used to determine ESPVR and PRSW, and an exponential fit was used to calculate EDPVR.

### Pharmacokinetics—Tadalafil and Saxagliptin

Dosing for both treatments was determined through dedicated pharmacokinetic studies in a separate group of farm pigs for saxagliptin and Yucatan miniature swine for tadalafil. Saxagliptin was administered orally at doses of 10, 15, or 30 mg·kg<sup>-1</sup> and both drug levels and DPP-4 activity were assessed in plasma collected at 0.25, 0.5, 0.75, 1, 1.5, 2, 4, 6, 8, and 24 hours postdosing. A dose of 10 mg·kg<sup>-1</sup> resulted in at least 85% inhibition of DPP-4 activity at 24 hours. Subsequent steady-state trough levels obtained in the HF-SAX group confirmed that the 10 mg·kg<sup>-1</sup> dose of saxagliptin once daily maintained at least 85% inhibition of DPP-4 activity. Tadalafil was administered orally at doses of 1, 3, and 8 mg·kg<sup>-1</sup> and blood samples were collected at 0.25, 0.5, 0.75, 1, 1.5, 2, 4, 24, 48, and 72 hours post oral dosing. Each dose level was administered to the same study animal at 7-day intervals for 3 successive weeks. Although a direct correlation of plasma concentrations with efficacy has not been established, a total tadalafil plasma concentration of 55 ng/mL (≈90% enzyme inhibition *in vitro*) constitutes a reasonable pharmacodynamic target for clinical development.<sup>20</sup> Plasma tadalafil levels were modeled, and a dose of 2 mg·kg<sup>-1</sup> twice/day (total 4 mg·kg<sup>-1</sup>·day<sup>-1</sup>) was chosen as plasma steady-state trough levels >50 ng/mL were confirmed in all animals.

### Transthoracic M-Mode and 2-Dimensional Speckle Tracking Echocardiography

Transthoracic echocardiography was performed with animals under telazol/xylazine sedation (2.25/1.12 mg·kg<sup>-1</sup>) in the supine/right lateral position 6 months postbanding as previously described.<sup>17–19</sup> Short-axis 2-dimensional M-mode images were recorded at the midpapillary level using a GE Vivid I Ultrasound system with a 2.5-MHz transducer, and all analyses were performed offline using GE EchoPac Software. LV chamber dimensions including LV internal diastolic dimension (LVIDd), LV internal systolic dimension, LV wall thickness (LV systolic wall thickness; LV diastolic wall thickness, LV WTd), and interventricular septum wall thickness (interventricular septum systolic wall thickness, IVS WT<sub>s</sub>; interventricular septum diastolic wall thickness, IVS WT<sub>d</sub>) were calculated from M-mode recordings. Relative wall thickness (normalized to LVIDd) was calculated as (LV WT<sub>d</sub>+IVS WT<sub>d</sub>)/LVIDd×1000. Six segments of the LV and septum were generated from apical 4-chamber and short-axis 2-dimensional views (acquired at the mitral-valve and apex

levels) and averaged to determine global strain, strain rate, and displacement in the longitudinal, radial, and circumferential directions over 3 cardiac cycles using 2-dimensional speckle tracking.<sup>17,18,21</sup> Torsion was calculated as the difference between mitral and apical end-systolic rotation (degrees) and normalized to both LV hypertrophy (wall thickness) and end-diastolic chamber length as previously described.<sup>17,22</sup>

### Cardiomyocyte Morphology and Functional Measures

LV cardiac myocytes were enzymatically isolated from LV wedge preparations of excised hearts as previously described.<sup>16,23</sup> Experiments monitoring cardiomyocyte contractile activity simultaneously with [Ca<sup>2+</sup>]<sub>i</sub> were performed at 34°C to 36°C using an IonOptix Calcium and Contractility Recording System (IonOptix, Milton, MA). Myocytes were loaded with fluo-4/AM (5 μmol/L fluo-4 AM for 10 minutes, 40–60-minute wash) and superfused with physiological saline solution containing (in mmol/L): 135 NaCl, 5 KCl, 2 CaCl<sub>2</sub>, 1 MgCl<sub>2</sub>, 10 D-glucose, 10 HEPES, 1 NaHCO<sub>3</sub>, pH 7.4 with NaOH. Action potentials (0.25, 0.5, and 1 Hz) were induced using electrical field stimulation (S48; Grass Instruments, Warwick, RI) with platinum electrodes placed at the edges of the bath. Action potential-induced Ca<sup>2+</sup> transients and L<sub>s</sub> shortening were analyzed offline using Ionwizard 6.3 software (IonOptix) with the following parameters assessed: (1) Ca<sup>2+</sup> transient amplitude (ΔF/F<sub>0</sub>, where F<sub>0</sub> is the fluorescence prior to the Ca<sup>2+</sup> transient and ΔF=F<sub>peak</sub>-F<sub>0</sub>); (2) Diastolic sarcomere length; and (3) Shortening amplitude (L<sub>0</sub>-L), where L<sub>0</sub> is the diastolic sarcomere length and L is the sarcomere length at shortening nadir. Values of 4 to 6 consecutive steady-state transients were obtained and averaged to obtain a single average value for each parameter per cell per experimental trial. For cell morphology measurements, cardiomyocytes were incubated in Ca<sup>2+</sup>-free physiological saline solution supplemented with 1 mmol/L EGTA and 20 mmol/L 2,3-butanedione monoxime. Transmitted light images were obtained (1024×1024 pixels, 0.22 μm per pixel) and length and width were defined as the longest internal dimension perpendicular to (length) and parallel to (width) sarcomere striations.

### Protein Levels

Western blot analysis was used to determine protein levels as previously described<sup>6,16,19,24</sup> in buffer containing 150 mmol/L NaCl, 10 mmol/L Tris pH 7.4, 1 mmol/L EDTA, 1% Triton X-100, and protease/phosphatase inhibitors (Halt, Thermo Scientific). After sonication, the lysates were centrifuged at 17 000g for 10 minutes to remove insoluble material and

sample concentration was then determined by Bradford assay (Bio-Rad). Equal amounts of protein in SDS loading buffer were run on 10% SDS-PAGE gels before transfer to polyvinylidene difluoride (PVDF) membranes. After blocking in 10% nonfat milk primary antibodies, Akt (60 kDa; Cell Signaling Technologies, 1:500), phospho-Akt (60 kDa, Ser 473; Cell Signaling Technologies, 1:500), ERK1/2 (42 and 44 kDa; Cell Signaling Technologies, 1:500), phospho-ERK1/2 (42 and 44 kDa, Thr 202/Thr 204; Cell Signaling Technologies, 1:500), SAPK/JNK (46 kDa; Cell Signaling Technologies, 1:500), phospho-SAPK/JNK (46 and 54 kDa, Thr 183/Thr 185; Cell Signaling Technologies, 1:500), OxPhos antibody cocktail (Abcam, ab110413, 1:1000), cyclophilin-D (41 kDa; Abcam, ab110324, 1:1000), mitochondria phosphate carrier (40 kDa; custom made by YenZym, 1:1000), adenine nucleotide translocase-1/2 (33 kDa; Santa Cruz, Sc-9299, 1:1000), voltage-dependent anion channel (31 kDa; Abcam, ab14734, 1:1000), PDE5 (100 kDa; Cell Signaling, 1:1000 dilution), and anti-clyceraldehyde-3-phosphate dehydrogenase (37 kDa; Millipore, 1:1000) were applied to the membranes. The appropriate alkaline phosphatase-conjugated secondary antibodies (Cell Signaling, 1:1000) were then applied to the membrane prior to imaging on a Bio-Rad Gel Doc XR using chemifluorescence (GE Healthcare Life Sciences).

### Atrial/BNP and Neuropeptide Y (NPY) Plasma Levels

Plasma atrial natriuretic peptide (ANP) and BNP were measured as previously described.<sup>25–27</sup> Blood was drawn into EDTA tubes and chilled until centrifuged at 750 *g* for 10 minutes at 4°C. One milliliter of plasma was aliquoted into 12×75-mm polystyrene tubes and frozen until assayed. One milliliter of plasma was extracted using C-18 Bond Elut cartridges. After washing cartridges with 4 mL 100% methanol and 4 mL water, plasma was applied and cartridges were washed again with 2 mL saline, 6 mL water, and 1 mL 100% methanol. ANP was eluted with 2 mL 75% methanol and 1% trifluoroacetic acid. Eluates were dried/concentrated on a Savant speed vac overnight, and resuspended in 300 μL assay buffer. One hundred microliters of standards and samples were incubated with 100 μL diluted (1:150 000) anti-human ANP (Phoenix Pharmaceuticals, Mountain View, CA) at 4°C. After 18 hours, 100 μL (10 000 counts) I<sup>125</sup>-labeled ANP is added and incubated at 4°C. After 18 hours incubation, a second antibody was added to all samples to separate the free and bound fractions. Samples were centrifuged, the free fraction was aspirated, and the bound fraction was counted on a gamma counter. A standard curve was generated and used to calculate the concentrations of the unknown samples and reported in pg/mL. The range of

the standard curve is 2 to 500 pg/mL. Inter- and intra-assay variability was 9% and 6%, respectively. Recovery of 64 pg was 81±2%. Cross-reactivity was <1% with N-ANP, BNP, C-type natriuretic peptide (CNP), endothelin, and adrenomedullin.

BNP was eluted from the cartridges with 2 mL of 90% methanol in 1% trifluoroacetic acid. Samples were dried on a Savant Speed Vac concentrator. The eluates were dried and reconstituted in 300 μL assay buffer. The radioimmunoassay used for this assay was a nonequilibrium assay from Phoenix Pharmaceuticals (Mountain View, CA) that uses an antibody to human, rat, or canine BNP. One hundred microliter standards or samples were incubated with 100 μL diluted antibody for 18 to 24 hours at 4°C. After incubation, 10 000 counts of iodinated (I<sup>125</sup>) BNP were added and incubated at 4°C. After 18 hours incubation, 100 μL of second antibody (goat anti-rabbit) and 100 μL normal rabbit serum were added to all samples to separate the free and bound fractions. After 1.5-hour room temperature incubation, samples were centrifuged, the free fraction was aspirated, and the discarded and bound fraction was counted on a gamma counter. A standard curve was generated and used to calculate the concentrations of the unknown samples and reported in pg/mL. The range of the standard curve was 0.5 to 128 pg/mL, recovery was 73%, and inter- and intra-assay variability was 11% and 7%, respectively. There was no cross-reactivity with ANP, CNP, or endothelin-1,2,3.

NPY was eluted similarly to BNP. After resuspension in 500 μL assay buffer, 100 μL of standards and unknown samples were incubated with 100 μL rabbit-anti human NPY at 4°C overnight. After 18 hours incubation, 100 μL I<sup>125</sup>-labeled antigen is added and incubated overnight at 4°C. The range of the standard curve was 5 to 1280 pg/mL, recovery was 78%, and intra-assay variability was 10%. There was no cross-reactivity with ANP, BNP or CNP, and 100% cross-reactivity with human NPY and peptide YY.

### cGMP-PKG-PDE5 Activity and Protein Levels

Myocardial cGMP levels for flash-frozen LV samples were examined using a commercial EIA kit (Amersham) as previously described.<sup>6,24</sup> The LV samples were homogenized in 6% trichloroacetic acid, centrifuged, and extracted with water-saturated diethyl ether. The aqueous phase was transferred, lyophilized, and the pellet resuspended in 200 μL of lysis buffer. The dissolved samples were acetylated with 20 μL of acetylation reagent, and then 50 μL of each sample were incubated with 100 μL of antiserum in a 96-well plate at 4°C. After 2 hours, 100 μL of diluted conjugate were added and incubated for 1 hour at 4°C. After washing, 200 μL of room temperature equilibrated enzyme substrate (tetramethylbenzidine) were added immediately and incubated for 30 minutes at room



temperature with shaking. The color was quantified at 630 nm by spectrophotometry, and cGMP levels were normalized by total protein concentration measured by bicinchoninic acid method (Pierce).

In vitro PKG activity was assayed in frozen LV samples, in the presence of cGMP and ATP, which were allowed to phosphorylate the bound substrate using a colorimetric assay kit (Cyclex) as previously described.<sup>6,24</sup> Ten microliters (30  $\mu$ g protein) of each sample, including PKG positive control and 90  $\mu$ L of kinase reaction buffer containing cGMP and ATP, were incubated in a 96-well plate for 30 minutes at 30°C. After washing, 100  $\mu$ L of horseradish peroxidase conjugated detection antibody (10H11) were added and incubated at room temperature. After 1 hour, each sample was washed and incubated with 100  $\mu$ L of chromogenic substrate tetramethylbenzidine at room temperature. After 10 minutes, 100  $\mu$ L of stop solution was added to each well, and the color was quantified at dual wavelengths of 450/540 nm by spectrophotometry.

In vitro PDE5 activity was assessed by fluorescence polarization assay (Molecular Probes) as previously described.<sup>6,24</sup> LV samples were homogenized in lysis buffer (Cell Signaling), and 1  $\mu$ L (3  $\mu$ g) of each sample was incubated with 19  $\mu$ L of reaction buffer containing 1 mmol/L dithiothreitol and 200 nmol/L cGMP at room temperature. After 1 hour, 60  $\mu$ L of Immobilized metal ion affinity-based fluorescence polarization binding solution were added and incubated up to 2 hours. The fluorescence polarization was measured at 485 nm by spectrophotometry.

### DPP-4 Assay

DPP-4 activity was measured at 25°C and monitored using a Shimadzu UV1650PC UV/Visible Spectrophotometer in conjunction with a Shimadzu 6-cell CPS temperature-controlled sample conveyor system. Chemical constituents of the 1-mL assay included the following: 500  $\mu$ L 2X ATE (104 mmol/L ACES, 104 mmol/L Tris, and 208 mmol/L ethanolamine adjusted to pH 7.4 with 5 mol/L HCl), 500  $\mu$ L 2 mmol/L substrate (Gly-Pro-*p*-nitro aniline), and 50  $\mu$ L of serum or plasma. Negative enzyme controls were set up similarly using heat-inactivated serum or plasma. A standard curve was established under the same buffer and measurement conditions using serial 2-fold dilutions of *p*-nitro-aniline (800  $\mu$ mol/L to 3.13  $\mu$ mol/L product).

### Mitochondrial Isolation, Swelling, Ca<sup>2+</sup> Retention Capacity, and Respiration

The isolation of cardiac mitochondrial and cytosolic fractions was carried out as previously described.<sup>16,19</sup> Briefly, LV tissue was homogenized using a Dounce homogenizer in

buffer containing 250 mmol/L sucrose, 10 mmol/L Tris pH 7.4, and 1 mmol/L EDTA. The homogenate was then centrifuged at 1000g for 5 minutes to pellet nuclei and unbroken cells/debris. The supernatant was then centrifuged at 10 000g for 10 minutes to pellet mitochondria, which were subsequently washed twice in EDTA-free homogenization buffer. Mitochondrial swelling, Ca<sup>2+</sup> retention capacity, and respiration procedures were performed as described previously.<sup>16,19</sup> Briefly, cardiac mitochondria were resuspended in buffer containing (in mmol/L): 120 KCl, 5 KH<sub>2</sub>PO<sub>4</sub>, and 10 Tris pH 7.4 with mitochondrial protein quantified by Bradford assay. Swelling was induced in 0.2 mg/mL mitochondria by the addition of CaCl<sub>2</sub> (10–100  $\mu$ mol/L) and measured spectrophotometrically at 520 nm. That the mitochondrial permeability transition (MPT) pore was responsible for the swelling response was confirmed by preincubating the mitochondria with 1  $\mu$ mol/L of the MPT inhibitor cyclosporine-A for 5 minutes prior to the addition of Ca<sup>2+</sup>. For Ca<sup>2+</sup> retention capacity, 0.1 mg/mL mitochondria were energized with 5 mmol/L succinate, and 20  $\mu$ mol/L EDTA and 1  $\mu$ mol/L Ca<sup>2+</sup>-green 5N (Life Technologies) were added to the suspension and fluorescence monitored (500ex, 530em). Sequential pulses of 5  $\mu$ mol/L CaCl<sub>2</sub> were then added each minute until a large fluorescence increase, derived from MPT pore-induced Ca<sup>2+</sup> release, was detected. Mitochondrial oxygen consumption was measured using a Clark-type electrode in buffer supplemented with 1 mmol/L MgCl<sub>2</sub> and either 5 mmol/L glutamate and 5 mmol/L malate (Complex I) or 10 mmol/L succinate (Complex II). Following the addition of 0.125 mg/mL mitochondria to the cuvette, State 2 (resting state) was recorded. State 3 was initiated by adding 0.2 mmol/L ADP to the reaction mixture. Oligomycin (1  $\mu$ mol/L) was then added to the suspension to induce State 4. Respiratory control, as determined by the State3/State2 and State3/State4 rate ratios, was then determined.

### Histology and Immunohistochemistry

Cross sections of LV were formalin fixed, embedded in paraffin, and stained for assessment of collagen as previously published.<sup>16,19</sup> Briefly, total collagen was visualized using Picrosirius red staining and quantified from 4 separate fields/animal using Image-Pro Plus analysis software (MediaCybernetics, version 6.2, Bethesda, MD) and expressed as the percent area stained.

### Statistical Analysis

All data analysis was performed using SigmaPlot version 12.3 (SysStat Software Inc., San Jose, CA). Treatment comparisons were made using either repeated-measures ANOVA

(RM-ANOVA) or 1-way ANOVA. Normality (Shapiro–Wilk’s test) and equality of variance were confirmed prior to comparison by ANOVA. Linear regression was used to examine the relationship between collagen and NPY levels. Group differences revealed by ANOVA were found using Student–Newman–Keuls post hoc analysis. All data are means±SE, and significance is reported at the  $P<0.05$  level.

## Results

### cGMP-PKG-PDE5, DPP-4, BNP, and ANP Levels/Activity

LV cGMP-PKG-PDE5 protein levels and activity relative to CON animals are presented in Figure 1A through 1E. Chronic treatment with the PDE5 inhibitor, tadalafil, significantly

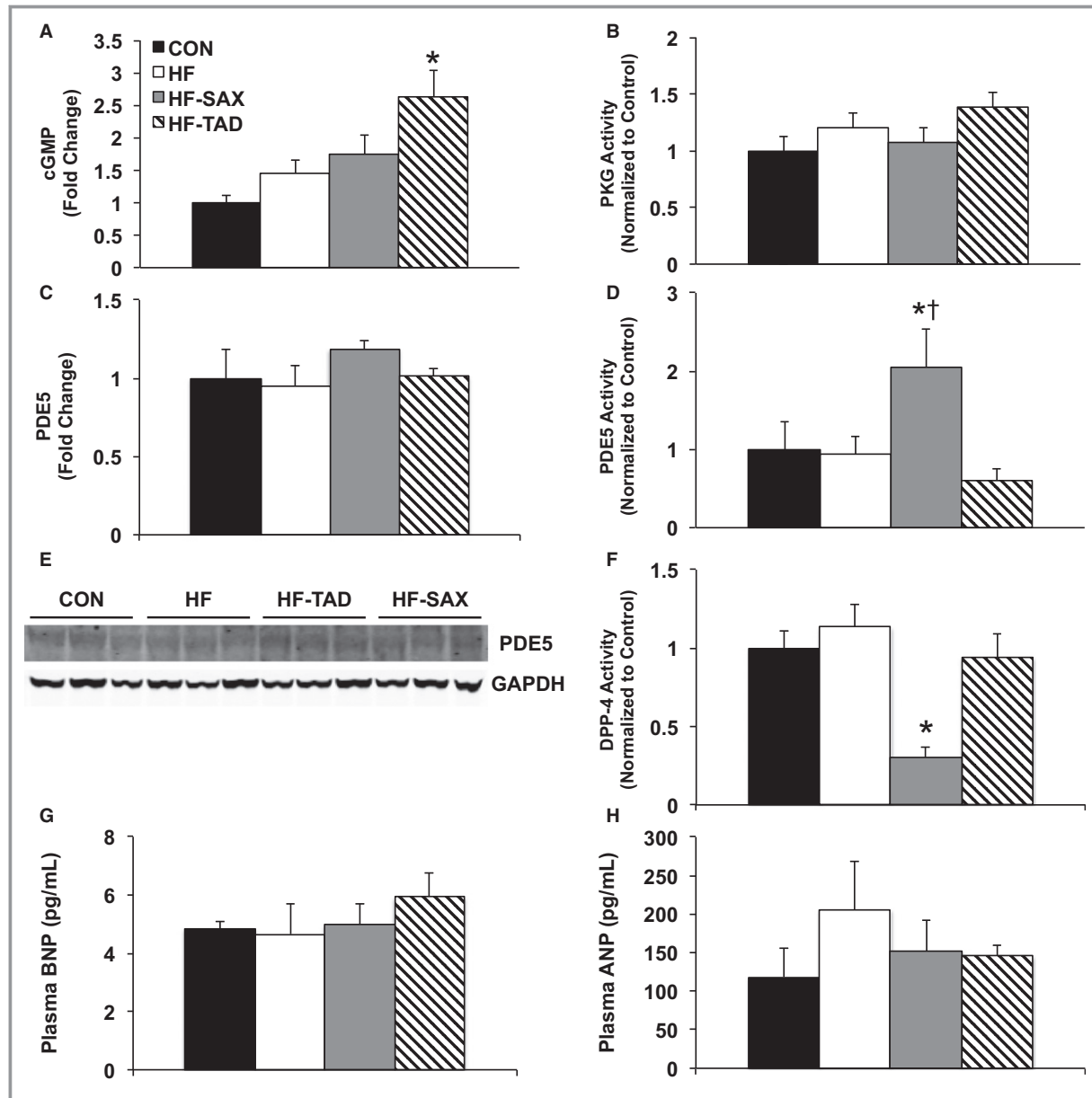


**Figure 1.** Left ventricular cGMP-PKG-PDE5, DPP-4, and plasma BNP and ANP levels and activity. A, cGMP level was significantly increased following treatment with tadalafil ( $*P<0.05$  vs CON, HF, and HF-SAX). B, PKG activity was unchanged by any treatment effect. C, PDE5 protein level was unaltered by heart failure. D, Saxagliptin increased PDE5 activity compared to all other groups ( $*P<0.05$  vs CON and HF-TAD,  $†P=0.058$  vs HF). E, Representative Western blot of PDE5 levels. GAPDH is presented to demonstrate equivalent loading conditions. F, Treatment with saxagliptin decreased plasma DPP-4 activity compared to CON ( $*P<0.05$  vs CON). Heart failure had no effect on DPP-4 activity. G and H, Plasma BNP (G) and ANP (H) levels were unchanged in aortic-banded groups irrespective of treatment compared to CON animals. ANP, atrial natriuretic peptide; BNP, brain natriuretic peptide; cGMP indicates cyclic guanosine monophosphate; CON, control; DPP-4, dipeptidyl-peptidase 4; HF, heart failure; PDE5, phosphodiesterase-5; PKG, protein kinase G; SAX, saxagliptin; TAD, tadalafil.

increased cGMP levels (Figure 1A) compared to the CON, HF, and HF-SAX groups. Increased cGMP in HF-TAD animals did not translate into increased PKG activity, its principal downstream effector kinase (Figure 1B). PDE5 protein levels were unchanged in HF or following either treatment arm (Figure 1C; representative Western blot Figure 1E); however, saxagliptin increased PDE5 activity (Figure 1D) compared to all other groups. DPP-4 activity was significantly decreased  $\approx 70\%$  from CON levels (Figure 1F), indicating our saxagliptin treatment was successful. No significant differences in plasma BNP (Figure 1G) or ANP (Figure 1H) levels were observed between groups.

## Cardiac Remodeling

Body weight was significantly increased in the HF-TAD group; therefore, heart and lung morphology measures were normalized to body weight and presented in Table 1. Global cardiac hypertrophy occurred to a similar extent in all aortic-banded groups, regardless of treatment. Increased lung weight:body weight ratio (indicative of pulmonary congestion) was observed only in the HF group compared to CON. Lung weight:body weight ratio was similar to CON animals in the HF-TAD and HF-SAX groups, suggesting these treatments were effective in preventing a clinical symptom of HF.

Representative histological sections of the LV from CON, HF, HF-SAX, and HF-TAD groups are shown in Figure 2A. Total

**Table 1.** Group Weight and Postmortem Assessment of Heart, Lung, and Cardiomyocyte Morphology

	CON	HF	HF-SAX	HF-TAD
<b>Gross morphology</b>				
Body weight, kg	30 $\pm$ 1	29 $\pm$ 2	30 $\pm$ 1	34 $\pm$ 1* <sup>†</sup>
HW:BW, g/kg	5.0 $\pm$ 0.1	6.1 $\pm$ 0.1*	5.9 $\pm$ 0.2*	5.8 $\pm$ 0.3*
Lung:BW, g/kg	7.1 $\pm$ 0.2	8.3 $\pm$ 0.4*	7.6 $\pm$ 0.2	6.6 $\pm$ 0.3 <sup>‡</sup>
LV+S:BW, g/kg	3.3 $\pm$ 0.1	3.9 $\pm$ 0.1*	3.8 $\pm$ 0.1*	3.7 $\pm$ 0.2*
RV:BW, g/kg	1.0 $\pm$ 0.1	1.3 $\pm$ 0.1 <sup>§</sup>	1.2 $\pm$ 0.1 <sup>§</sup>	1.2 $\pm$ 0.1 <sup>§</sup>
Atria:BW, g/kg	0.7 $\pm$ 0.1	0.9 $\pm$ 0.1*	0.9 $\pm$ 0.1*	0.9 $\pm$ 0.1*
<b>Cardiomyocyte morphology</b>				
Length, $\mu$ m	164 $\pm$ 3	170 $\pm$ 2	168 $\pm$ 2	177 $\pm$ 3* <sup>†</sup>
Width, $\mu$ m	29 $\pm$ 1	34 $\pm$ 1*	31 $\pm$ 1	40 $\pm$ 1* <sup>†</sup>
Length:width ratio	6.0 $\pm$ 0.2	5.6 $\pm$ 0.2*	6.1 $\pm$ 0.2	5.1 $\pm$ 0.2* <sup>†</sup>

Values are means $\pm$ SE. Cardiomyocyte morphology, CON: n=6 animals, 180 cells; HF: n=7 animals, 209 cells; HF-SAX: n=7 animals, 210 cells; HF-TAD: n=8 animals, 198 cells. Atria:BW indicates right+left atria weight:body weight ratio; CON, control; HF, heart failure; HW:BW, heart weight:body weight ratio; LV+S:BW, left ventricle+septum weight:body weight ratio; RV:BW, right ventricle weight:body weight ratio; SAX, saxagliptin; TAD, tadalafil.

Significance is indicated at \* $P$ <0.05 vs CON; <sup>†</sup> $P$ <0.05 vs HF and HF-SAX; <sup>‡</sup> $P$ <0.05 vs HF and HF-SAX; <sup>§</sup> $P$ =0.06 vs CON.

collagen levels (Picrosirius red staining; expressed as the percent area of LV stained), indicative of increased fibrosis, was significantly increased in HF animals compared to CON (Figure 2B). Treatment with either saxagliptin or tadalafil prevented aortic banding–induced increases in LV collagen content. Circulating plasma NPY levels were increased in HF compared to CON animals (Figure 2C). Cumulative group data, indicated by the regression line, showed LV collagen content was positively correlated with NPY (Figure 2D). Increased plasma NPY levels and the rightward shift in NPY in relation to collagen were attenuated by both saxagliptin and tadalafil (Figure 2C and 2D). Fibrotic remodeling was not associated with any changes to Akt, ERK, or SAPK/JNK signaling, as no differences in the respective protein phosphorylation levels were detected (Figure 2E and 2F).

Assessment of LV morphology via echocardiography supports our postmortem data (Table 2). Aortic banding increased diastolic wall thickness, primarily in the interventricular septal wall (IVS Wtd), but did not alter LV internal diastolic dimension (LVIDd) compared to CON irrespective of treatment. Relative wall thickness (normalized to LVIDd) was also significantly elevated in all aortic-banded groups. In total, these findings reflect concentric hypertrophic remodeling.

Isolated cardiomyocyte morphology was largely consistent with our postmortem and ultrasound findings (Table 1, CON: n=6 animals, 180 cells; HF: n=7 animals, 209 cells; HF-SAX: n=7 animals, 210 cells; HF-TAD: n=8 animals, 198 cells). Cell width was significantly increased in both HF and HF-TAD animals compared to the CON group, and cell length was also increased in HF-TAD animals. The decrease in length:width ratio observed in the HF and HF-TAD compared to CON reflects a classic cellular indicator of concentric hypertrophy. Cell width, length, and length:width ratio was the same in HF-SAX animals compared to the CON group.

## Systolic Function

Resting hemodynamic and LV functional data are presented in Table 3 (representative pressure-volume loops are shown in Figure 3). Heart rate and end-systolic pressure were the same among all groups. End-systolic volume was decreased in both the HF and HF-TAD groups and unchanged in HF-SAX animals compared to CON. LV ejection fraction and stroke volume were equivalent in all groups, demonstrating preserved systolic function at rest in the presence of clinical markers of HF (ie, lung congestion, a hallmark feature of HFpEF). Similar to previous observations in our swine model and human HFpEF,<sup>1,2,23</sup> LV contractility (measured as ESPVR and PRSW) was significantly increased in HF animals compared to the CON group. Tadalafil did not prevent aortic banding–induced increases in LV contractility and actually increased

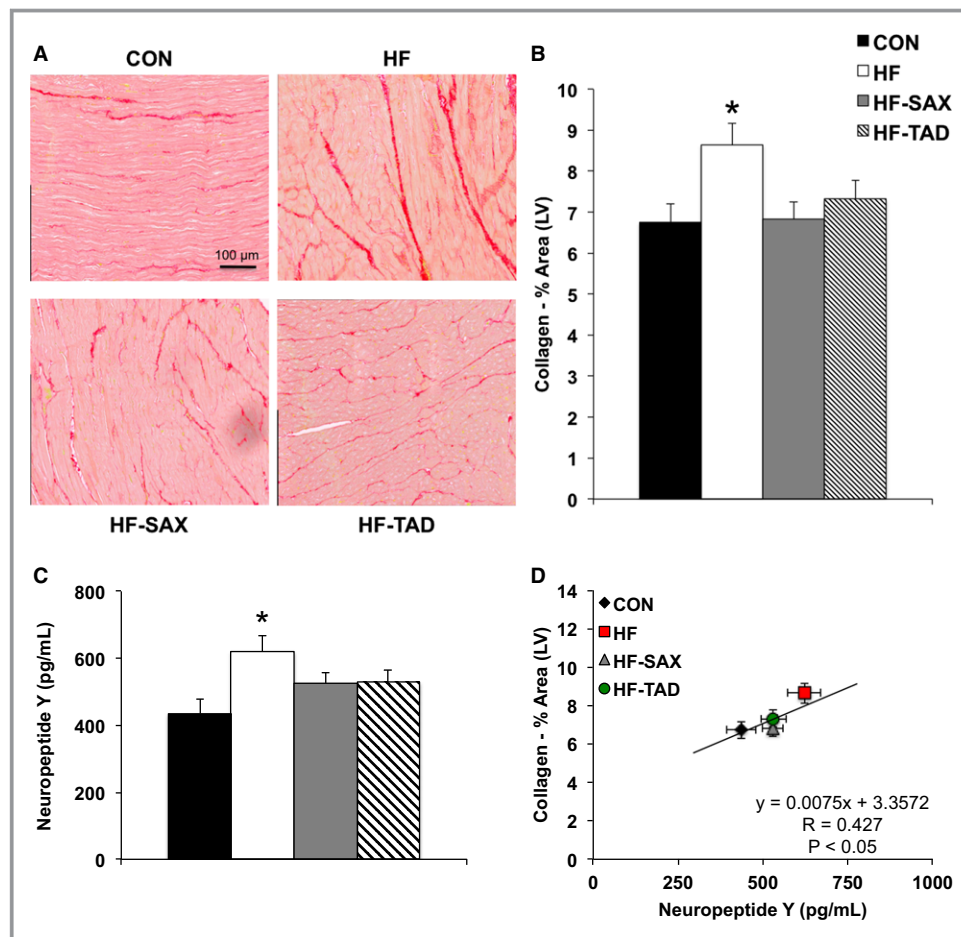


**Figure 2.** Left ventricular collagen deposition. A, Representative histological sections of Picrosirius red-stained LV showing increased fibrosis in the HF group compared to CON. Magnification:  $\times 40$ . B, Both saxagliptin and tadalafil prevented the aortic banding-induced increase in total collagen deposition ( $*P < 0.05$  vs CON). C, Increased NPY levels in HF compared to CON animals were attenuated in the HF-SAX and HF-TAD groups ( $*P < 0.05$  vs CON). D, Linear regression demonstrating a significant correlation between total collagen and NPY. Both saxagliptin and tadalafil attenuated the right upward shift in the relationship observed in HF animals. E, Left ventricular Akt, ERK, and SAPK/JNK protein levels 6 months post-aortic-banding. There were no differences in activated protein levels (expressed as the ratio of phosphorylated to total protein) of Akt, ERK, or SAPK/JNK in aortic-banded animals regardless of treatment compared to the CON group. F, Representative Western blots of total and phosphorylated Akt, ERK 1/2, and SAPK/JNK protein levels. CON indicates control; ERK, extracellular signal-regulated kinase; HF, heart failure; LV, left ventricular; NPY, neuropeptide Y; SAX, saxagliptin; TAD, tadalafil.

PRSW above levels observed in the HF group. Saxagliptin partially attenuated this response, as ESPVR was significantly lower than the HF and HF-TAD groups and PRSW values were the lowest of the aortic-banded groups.

We also examined cell shortening (CON:  $n=6$  animals, 15 cells; HF:  $n=7$  animals, 24 cells; HF-SAX:  $n=6$  animals, 18 cells; HF-TAD:  $n=6$  animals, 11 cells) and calcium transients (CON:  $n=4$  animals, 10 cells; HF:  $n=7$  animals, 20 cells; HF-SAX:  $n=6$  animals, 13 cells; HF-TAD:  $n=6$  animals, 9 cells) in isolated LV cardiomyocytes paced at increasing frequencies (0.25, 0.50, and 1.0 Hz). Representative shortening and calcium transients from the CON group illustrating our experimental paradigm are

presented in Figure 4A. A negative shortening-frequency relationship, a cellular characteristic of HF,<sup>28</sup> was observed in the HF group compared to CON animals at absolute lengths (Figure 4B; group  $\times$  pacing interaction) and relative to 0.25 Hz (Figure 4C; group  $\times$  pacing interaction). Both saxagliptin and tadalafil prevented the aortic banding-induced negative shortening-frequency relationship. However, absolute shortening was significantly reduced from CON levels in the HF-TAD group at all pacing frequencies and at 0.5 and 1.0 Hz in the HF-SAX group. A parallel decrease in calcium transient amplitude (Figure 4D; group  $\times$  pacing interaction) was seen in the HF-TAD group compared to all other groups.



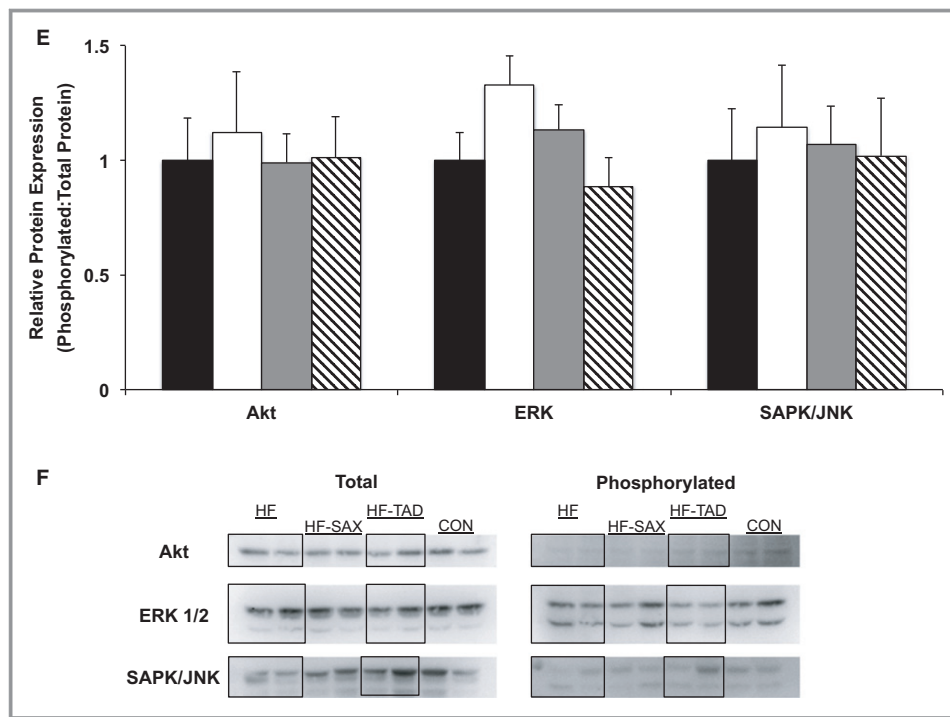


**Figure 2.** continued.

Aortic banding changed LV mechanics in a manner suggesting impaired systolic function. Representative 2-dimensional speckle tracking echocardiography images illustrating global longitudinal strain are shown in Figure 5A through 5D and demonstrate the decrease in global longitudinal strain (Figure 5E) observed in the HF group compared to CON. This effect was also seen in HF-SAX animals. Consistent with the cardiomyocyte shortening data presented in Figure 4B, systolic mechanics were impaired to a greater extent in the HF-TAD group as global longitudinal, circumferential, and radial strain were decreased compared to all other groups (Figure 5E). Torsion was preserved (Figure 5F) or increased (when normalized to cardiac remodeling; Figure 5G—septum, Figure 5H—LV) in HF compared to CON animals. The increase in normalized torsion observed in the HF group was prevented in both HF-TAD and HF-SAX animals.

### LV Diastolic Function

LV end-diastolic volume was decreased in HF and HF-TAD animals and unchanged in HF-SAX compared to the CON group (Table 3). End-diastolic pressure, although not considered pathological (>15 mm Hg), was significantly increased in the HF-TAD group compared to all other groups. The slope of the EDPVR was significantly increased in the HF compared to CON group and indicative of global LV diastolic dysfunction. Neither saxagliptin nor tadalafil prevented aortic banding-induced diastolic impairment.

As a cellular surrogate of diastolic function, changes to resting cardiomyocyte sarcomere length in response to increased frequency of stimulation were examined. A significant pacing-induced decrease in absolute (Figure 4E; group×pacing interaction) and relative to 0.25 Hz (Figure 4F;

**Table 2.** Left Ventricular Morphology—Echocardiography

	CON	HF	HF-SAX	HF-TAD
LVIDd, cm	5.0±0.2	4.6±0.1	4.5±0.1	4.6±0.1
LVIDs, cm	2.7±0.1	2.4±0.1	2.6±0.1	2.7±0.1
LV WTd, cm	0.49±0.04	0.58±0.03	0.54±0.05	0.60±0.03
LV WTs, cm	1.2±0.1	1.2±0.1	1.2±0.1	1.3±0.1
IVS WTd, cm	0.80±0.05	1.01±0.03*	0.95±0.03*	0.96±0.05*
IVS WTs, cm	1.5±0.1	1.6±0.1	1.4±0.1	1.5±0.1
Relative LV+IVS WTd	262±17	352±14*	327±15*	337±17*

Values are means±SE. IVS WTd indicates interventricular septum diastolic wall thickness; IVS WTs, interventricular septum systolic wall thickness; LV WTd, left ventricular diastolic wall thickness; LV WTs, left ventricular systolic wall thickness; LVIDd, left ventricular internal diastolic dimension; LVIDs, left ventricular internal systolic dimension; Relative LV+IVS WTd, left ventricular and septal diastolic wall thickness normalized to LVIDd calculated as (LV WTd+IVS WTd)/LVIDd×1000. Significance is indicated at \* $P$ <0.05 vs CON.

**Table 3.** Pressure-Volume Analysis of Resting Systolic and Diastolic Function

	CON	HF	HF-SAX	HF-TAD
<b>Systolic function</b>				
HR, beats/min	102±9	97±4	103±3	108±4
LV ESV, mL	42±6	21±4*	33±7	25±3*
LV ESP, mm Hg	62±4	69±4	69±5	77±7
LV EF, %	55±6	67±5	62±6	66±3
LV SV, mL	50±5	42±3	50±4	46±3
ESPVR, mm Hg/mL	5±1	13±1*	8±1 <sup>‡§</sup>	14±2*
PRSW, mm Hg	52±4	76±3*	69±5*	90±4* <sup>†</sup>
<b>Diastolic function</b>				
LV EDV, mL	92±2	63±3*	83±9 <sup>‡</sup>	70±5*
LV EDP, mm Hg	7±1	9±1	9±1	11±1* <sup>†</sup>
EDPVR, mm Hg/mL	0.011±0.001	0.021±0.002*	0.017±0.002*	0.021±0.002*

Values are means±SE. CON indicates control; EDPVR, end-diastolic pressure-volume relationship; ESPVR, end-systolic pressure-volume relationship; HF, heart failure; HR, heart rate; LV EDP, left ventricular end-diastolic pressure; LV EDV, left ventricular end-diastolic volume; LV EF, left ventricular ejection fraction; LV ESP, left ventricular end-systolic pressure; LV ESV, left ventricular end-systolic volume; LV SV, left ventricular stroke volume; PRSW, preload recruitable stroke work; SAX, saxagliptin; TAD, tadalafil. Significance is indicated at \* $P<0.05$  vs CON; <sup>†</sup> $P<0.05$  vs HF and HF-SAX; <sup>‡</sup> $P<0.05$  vs HF; <sup>§</sup> $P<0.05$  vs HF-TAD.

group×pacing interaction) diastolic sarcomere length was observed in the HF and HF-TAD groups compared to CON. This finding, indicative of impaired diastolic relaxation, was prevented by saxagliptin treatment.

Representative 2-dimensional speckle tracking echocardiography images illustrating early and late peak longitudinal diastolic strain rate are shown in Figure 6A through 6D. LV global longitudinal strain rate was reduced in HF compared to CON animals (Figure 6E), illustrating that LV mechanics associated with early diastolic filling were consistent with our LV and cellular data. Early diastolic mechanics were impaired to a greater degree following treatment with tadalafil, and evident as reduced global longitudinal (Figure 6E) and apical circumferential strain rate (Figure 6F) compared to both CON and HF animals. Saxagliptin prevented, and in some cases improved, alterations to early diastolic LV mechanics observed in the HF group. Decreased global longitudinal strain rate was attenuated in the HF-SAX group (Figure 6E), and apical circumferential strain rate (Figure 6F) and untwisting (Figure 6G) were increased above normal CON levels.

Global longitudinal strain rate during late diastole is presented in Figure 6H. Compared to CON, both HF and HF-TAD animals showed increased global longitudinal strain rate during late diastole. Saxagliptin prevented this increase, as late diastolic longitudinal strain rate was reduced below CON levels.

### LV Mitochondrial Function

Our results indicate evidence of early mitochondrial dysfunction. Using Complex I substrates (Figure 7A), respiratory

control, as measured by State3/State2 and State3/State4 ratios, remained unchanged in the various groups. However, using Complex-II substrates (Figure 7B), respiratory control was decreased in HF-TAD animals compared to the CON group, suggestive of respiratory uncoupling. In line with this result, previous work has shown that tadalafil can affect skeletal muscle citrate synthase, which along with Complex II constitutes a portion of Krebs cycle enzymes.<sup>29</sup> We next assessed MPT, another index of mitochondrial dysfunction. There were no modifications in expression of the proteins thought to comprise the MPT pore including mitochondrial Complex V, Complex I, cyclophilin-D, mitochondrial phosphate carrier, adenine nucleotide translocase, voltage-dependent anion channel, and Complex II (Figure 7C and 7D). Regarding indices of MPT, we did not observe any changes in calcium-induced mitochondrial swelling (Figure 7E). However, calcium-retention capacity, a more sensitive MPT index, was decreased in HF animals compared to the CON group (Figure 7F) and indicative of increased susceptibility to Ca<sup>2+</sup>-induced MPT. Interestingly, this decrease was not observed in HF-SAX or HF-TAD animals. Saxagliptin prevented aortic banding-induced mitochondrial dysfunction.

### Discussion

In this study, we examined the therapeutic effect of manipulating the cGMP signaling pathway on LV remodeling and function in aortic-banded mini-swine displaying key clinical characteristics of HFpEF. Two separate pharmacological methods were tested: (1) promoting cGMP synthesis with

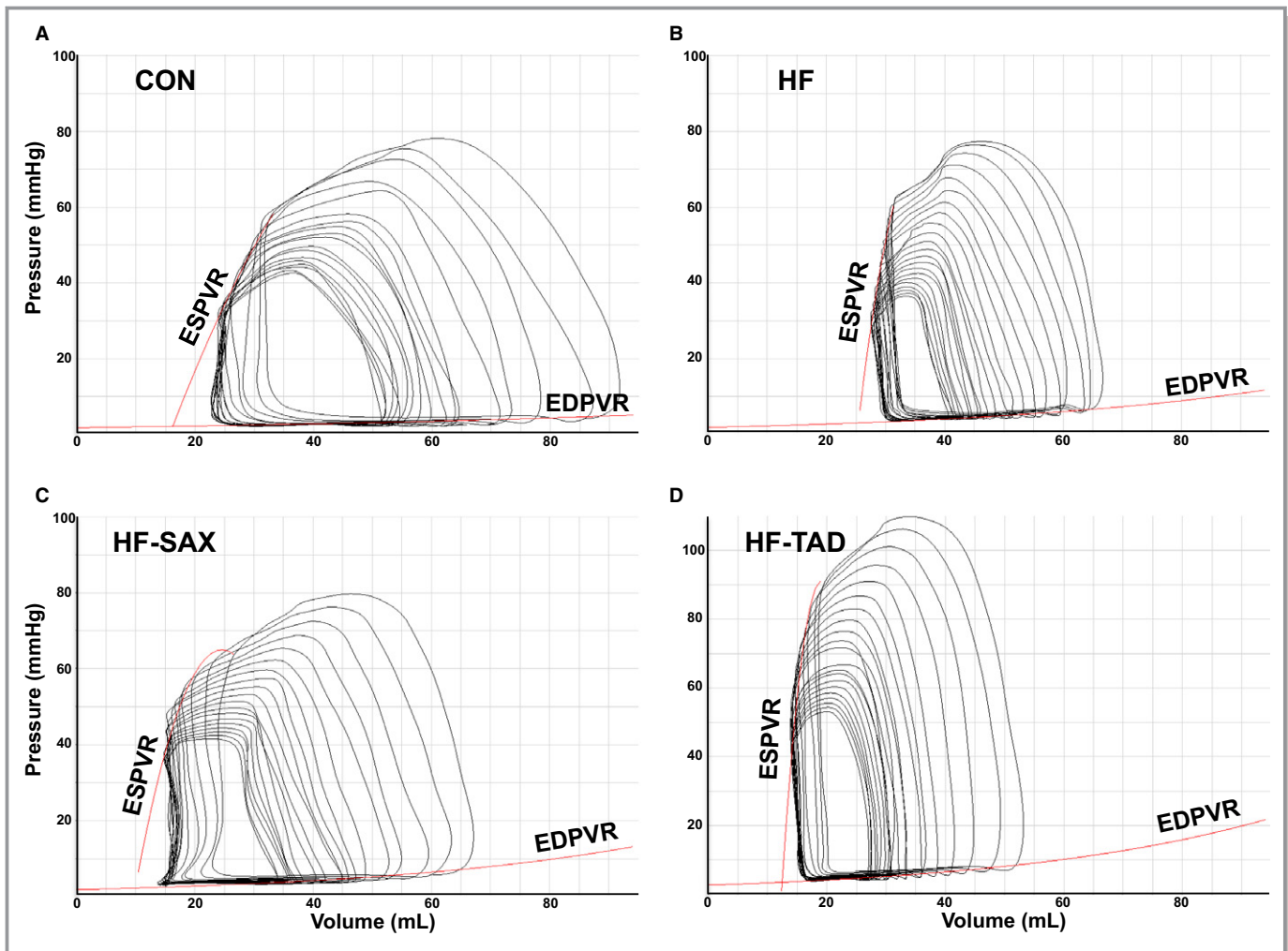


**Figure 3.** Representative P-V loops from individual CON (A), HF (B), HF-SAX (C), and HF-TAD (D) animals. CON indicates control; EDPVR, end-diastolic pressure-volume relationship; ESPVR, end-systolic pressure-volume relationship; HF, heart failure; P-V, pressure-volume; SAX, saxagliptin; TAD, tadalafil.

the DPP-4 inhibitor saxagliptin, and (2) preventing cGMP catabolism via the PDE5 inhibitor tadalafil. Our results show a number of novel findings: (1) increased LV collagen deposition observed in the HF group was attenuated by both drugs and correlated with circulating plasma NPY levels; (2) LV global and cellular function were distinctly altered in a drug-dependent fashion, with saxagliptin better preserving integrated LV systolic and diastolic function compared to tadalafil; and (3) although both drug treatments modified the cGMP-PKG-PDE5 signaling axis distinctly with saxagliptin increasing PDE5 activity and tadalafil increasing cGMP levels, neither resulted in a downstream increase in PKG activity.

Our data indicate saxagliptin and tadalafil had distinct effects on the LV functional profile that characterizes HFpEF, with saxagliptin providing the greatest benefit. As shown by our lab<sup>17,23</sup> and others,<sup>30–32</sup> aortic-banded swine develop significant LV hypertrophy. Regarding our hypothesis,

changes in cGMP levels and PDE5 activity following treatment with tadalafil or saxagliptin, respectively, did not limit LV hypertrophic remodeling in response to chronic pressure overload from a gross morphological perspective.

However, both saxagliptin and tadalafil prevented aortic banding–induced increases in LV collagen deposition, suggesting that treatment with either drug may limit detrimental and irreversible myocardial fibrosis. Drug-related prevention of LV fibrotic remodeling was significantly correlated with altered levels of a known DPP-4 substrate, neuropeptide Y (NPY). NPY levels are increased in disease states in which sympathetic nervous system activation is enhanced, such as diabetic or stress cardiomyopathy,<sup>33,34</sup> and our results show a significant increase in circulating plasma NPY in the HF group. Neuropeptide Y is positively correlated in humans with LV wall thickness, LV mass index, and associated with a higher risk of concentric hypertrophy.<sup>35,36</sup> A new study by Santos-Gallego

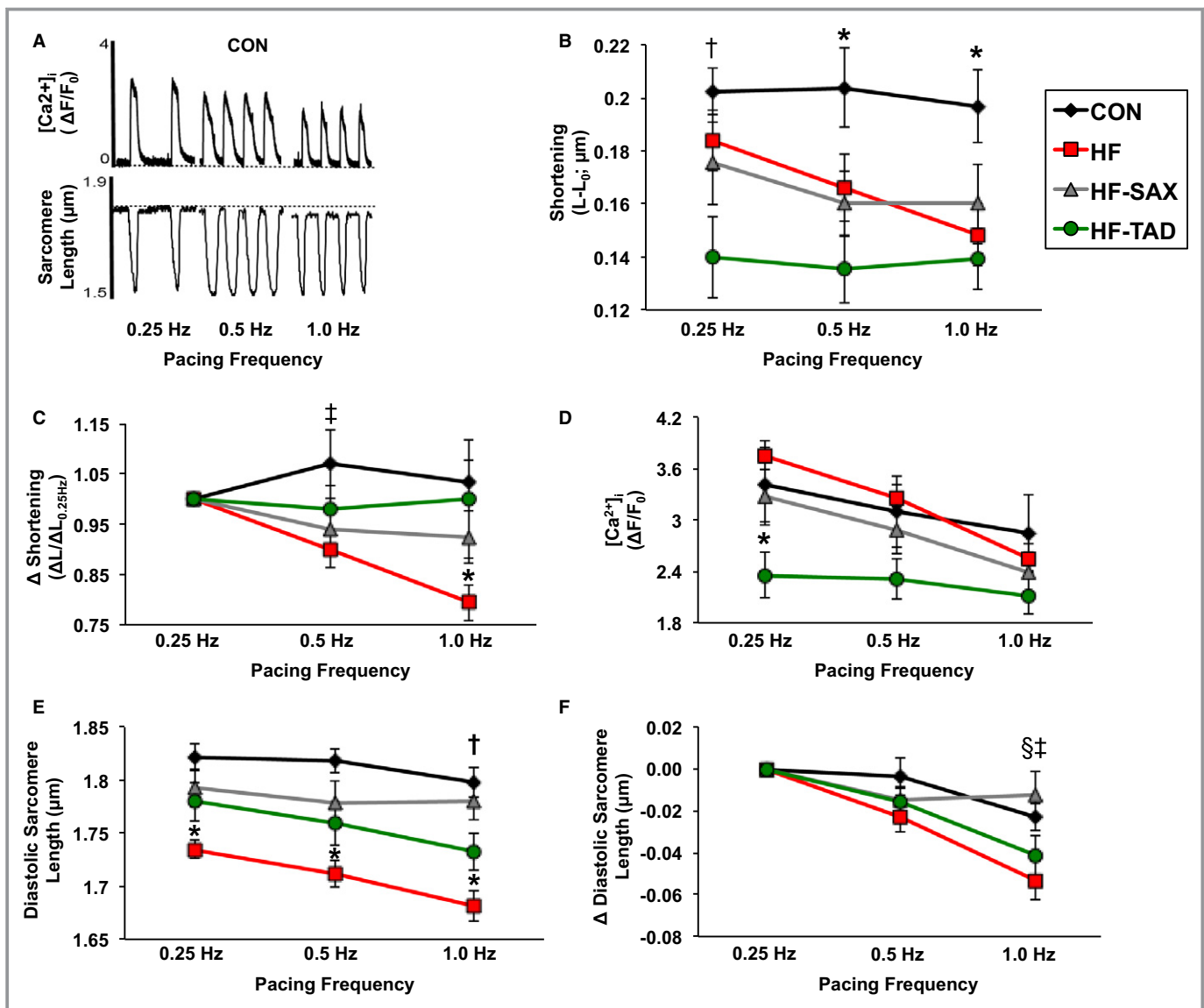


**Figure 4.** Cardiomyocyte frequency dependence of cell shortening/lengthening (CON: n=6 animals, 15 cells; HF: n=7 animals, 24 cells; HF-SAX: n=6 animals, 18 cells; HF-TAD: n=6 animals, 11 cells) and calcium transients (CON: n=4 animals, 10 cells; HF: n=7 animals, 20 cells; HF-SAX: n=6 animals, 13 cells; HF-TAD: n=6 animals, 9 cells). A, Representative calcium and sarcomere length traces at 0.25, 0.5, and 1.0 Hz from the CON group showing the experimental design. B and C, A negative shortening-frequency relationship was observed in the HF group compared to CON from an absolute (B, RM ANOVA group $\times$ pacing interaction,  $P < 0.05$ ; \* $P < 0.05$  vs all groups, † $P < 0.05$  CON vs HF-TAD) and relative perspective (C, normalized to 0.25 Hz, RM ANOVA group $\times$ pacing interaction,  $P < 0.05$ ; \* $P < 0.05$  HF vs all groups, ‡ $P < 0.05$  CON vs HF). D, Calcium  $[Ca^{2+}]_i$  transient amplitude ( $\Delta F/F_0$ ) was decreased in HF-TAD compared to all groups at 0.25-Hz pacing frequency (RM ANOVA group $\times$ pacing interaction,  $P < 0.05$ ; \* $P < 0.05$  HF-TAD vs all groups). E and F, Cardiomyocyte frequency dependence of cell lengthening represented by absolute (E) and relative (F; normalized to 0.25 Hz) diastolic sarcomere length. Saxagliptin preserves normal diastolic sarcomere length, which decreases significantly in response to increasing pacing frequency in the HF and HF-TAD groups compared to CON (RM ANOVA, group $\times$ pacing interaction,  $P < 0.05$ ; \* $P < 0.05$  HF vs all groups, † $P < 0.05$  CON vs HF-TAD, ‡ $P < 0.05$  HF vs CON and HF-SAX; § $P < 0.05$  HF-SAX vs HF-TAD). CON indicates control; HF, heart failure; SAX, saxagliptin; TAD, tadalafil.

et al showed that the involvement of Akt and ERK signaling is integral to cardiac remodeling in the remote myocardium of infarcted swine.<sup>37</sup> Our findings indicate pressure-overload-induced hypertrophy is not associated with changes to Akt or ERK activation and are similar to recent work demonstrating chronic NPY infusion induces diastolic dysfunction

and concurrent pathological cardiac hypertrophy, including increased fibrosis, independent of activated Akt/ERK signaling.<sup>38</sup> Based on our demonstrated inhibition of DPP-4 activity, NPY levels increased in the HF-SAX group as expected, although not to the pathologic levels observed in HF animals. Limited data support a role for PDE3 regulation of NPY in



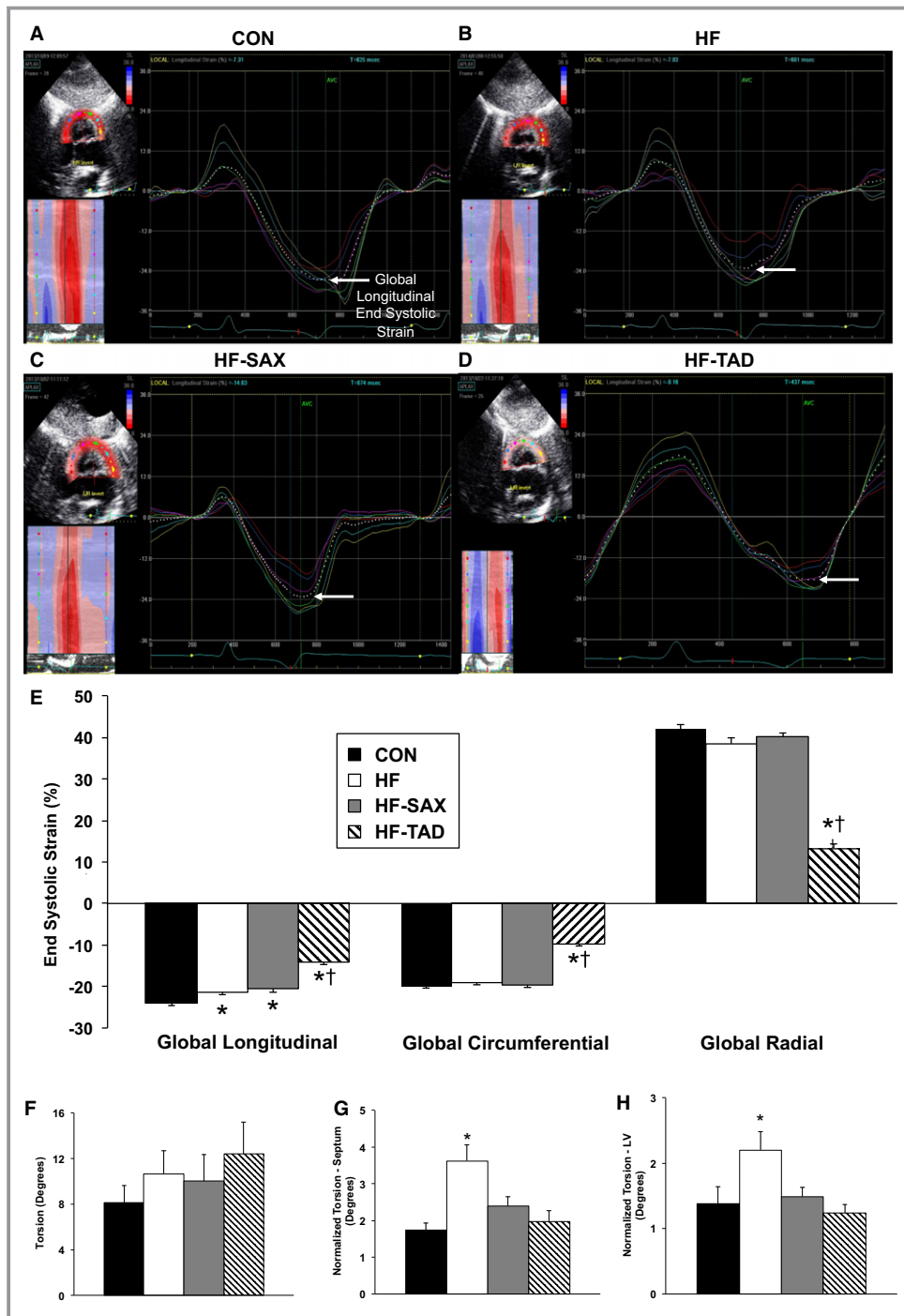


**Figure 5.** Global systolic LV strain and torsion. A through D, Representative 2DST echocardiography images from individual CON (A), HF (B), HF-SAX (C), and HF-TAD (D) animals highlighting decreased global longitudinal peak systolic strain in all aortic-banded groups (and to a greater extent in HF-TAD). E, Global longitudinal end-systolic strain was decreased in both HF and HF-SAX compared to the CON group. This effect of HF was enhanced in HF-TAD animals. Global circumferential and radial end-systolic strain was significantly decreased in HF-TAD animals compared to all other groups (\* $P < 0.05$  vs CON, † $P < 0.05$  vs HF and HF-SAX). F through H, LV torsion. There was no difference in absolute torsion between groups (F). Torsion normalized to chamber length and septum (G) or LV (H) remodeling was increased in HF animals compared to CON. This effect of heart failure was prevented in the HF-TAD and HF-SAX groups (\* $P < 0.05$  vs CON, HF-TAD, and HF-SAX) 2DST indicates 2-dimensional speckle tracking; CON, control; HF, heart failure; LV, left ventricular; SAX, saxagliptin; TAD, tadalafil.

hypothalamic neurons<sup>39</sup>; however, to the best of our knowledge this study is the first to demonstrate alteration of systemic NPY levels following chronic PDE5 inhibition. Our results suggest targeting of the NPY regulatory axis could hold therapeutic potential for limiting pathological fibrotic remodeling in heart failure.

We observed numerous indicators of diastolic dysfunction in the HF group at both the organ and cellular level. The current data and previous work from our lab support a mechanistic role for mitochondrial dysfunction, increased LV fibrosis, impaired calcium handling, and increased intrinsic cardiomyocyte stiffness regarding this dysfunction.<sup>16,18,19</sup> Interestingly, neither drug treatment prevented the aortic banding-induced increase in EDPVR despite inhibition of increased collagen deposition and maintenance of normal mitochondrial function by saxagliptin. This finding could be attributed to decreased phosphorylation of the large elastic cytoskeletal protein titin. Phosphorylation of titin by PKG decreases passive stiffness in cardiac myofibrils, and recent evidence has shown that increased passive stiffness in isolated cardiomyocytes from human HFpEF patients is associated with reduced cGMP levels and subsequent PKG activity.<sup>7–9</sup> Contrary to these findings, cGMP levels and PKG activity were unaltered in the HF group of the current study compared to CON. Combined with previous findings from our lab demonstrating titin isoforms do not shift in our model (ie, the N2BA:N2B ratio does not change),<sup>18</sup> we can reasonably speculate that increased titin stiffness as a result of decreased PKG activity was not a likely factor contributing to our results. Saxagliptin treatment did prevent pacing-induced decreases in resting cardiomyocyte sarcomere length and was associated with changes to LV mechanics considered beneficial during early and late diastole. The lack of enhanced mechanics associated with atrial systole in the HF-SAX group may be due to improved early diastolic mechanics related to passive filling, negating the need for augmentation of filling during late diastole.

From a systolic perspective, saxagliptin was also effective at preserving aspects of normal LV and cellular function. Although it did not prevent the reduced longitudinal systolic strain commonly observed in HFpEF patients,<sup>40–42</sup> which is known to correlate with higher LV filling pressures, lower cardiac output, and worse New York Heart Association functional class,<sup>40</sup> treatment with saxagliptin attenuated or prevented alterations to LV systolic function at the whole heart and cellular level observed in the HF group. Attenuation of the heightened contractile state often seen under resting conditions in HFpEF may be due to the preservation or improvement of normal LV diastolic cellular mechanics, myocardial collagen deposition, mitochondrial function, and cardiomyocyte diastolic function in HF-SAX animals despite an increase in the EDPVR. Thus, the combined effect of these

mechanisms in the HF-SAX group may be to preserve normal LV end-diastolic volume and diastolic filling, supporting optimal thick filament-to-thin filament geometry to sustain the Frank-Starling mechanism resulting in a normal systolic state (ie, the myocardium is not operating at “maximum” in order to maintain resting cardiac output). This idea is manifest in HFpEF as a loss of cardiac reserve in response to stress (eg, exercise, activities of daily living), which we have previously observed in this model.<sup>23</sup> Overall, our data show saxagliptin prevented HF-specific alterations to LV structure and function at the organ and cellular level that suggest cardiac output is protected by maintaining normal integration of systole and diastole during the cardiac cycle.

Changes to LV function observed following tadalafil treatment are more difficult to interpret. The HF-TAD group presented features of the “systolic paradox” often found in HFpEF including normal ejection fraction, stroke volume, and increased LV contractility (ESPVR and PRSW; shown by our lab<sup>23</sup> and others<sup>30</sup> in aortic-banded swine) in concert with reduced longitudinal, circumferential, and radial systolic mechanics. It is worthwhile to note that changes to systolic mechanics and cardiomyocyte function were greater than those observed in the HF group, implying systolic function may be more impaired in HF-TAD animals. It is reasonable to speculate that reductions in systolic strain following treatment with tadalafil may be a reflection of cellular processes promoting a more lusitropic state. However, if this were the case it is difficult to reconcile why strain rates during early diastole were reduced beyond levels observed in HF animals. Furthermore, increased late diastolic strain values equivalent to those observed in the HF group and pacing-induced diastolic dysfunction at the cellular level provide additional support of diastolic impairment in HF-TAD animals. Thus, it is unlikely tadalafil protected normal integrated cardiac function similar to that observed in the HF-SAX group. Rather, considered alongside early evidence of mitochondrial dysfunction, our functional and morphological data imply that treatment with tadalafil impaired diastolic function to a greater degree than observed in HF animals. In total, our data do not support the efficacy of tadalafil for improving cardiac dysfunction in HFpEF.

A primary strength of our study is the use of *in vivo* methodology in a large animal model that more closely mimics the human condition, providing translational impact. Less is known about cardiac signal transduction in large mammals, despite the significant differences between large and small mammalian hearts including life span, heart rate, Ca<sup>2+</sup> handling, tolerance for myocardial injury, and rate of progression of cardiac remodeling.<sup>43</sup> The differences in cardiac biology between small and large mammals are not purely academic. Originally, work from Takimoto et al<sup>6</sup> demonstrated the beneficial effects of PDE5 inhibition

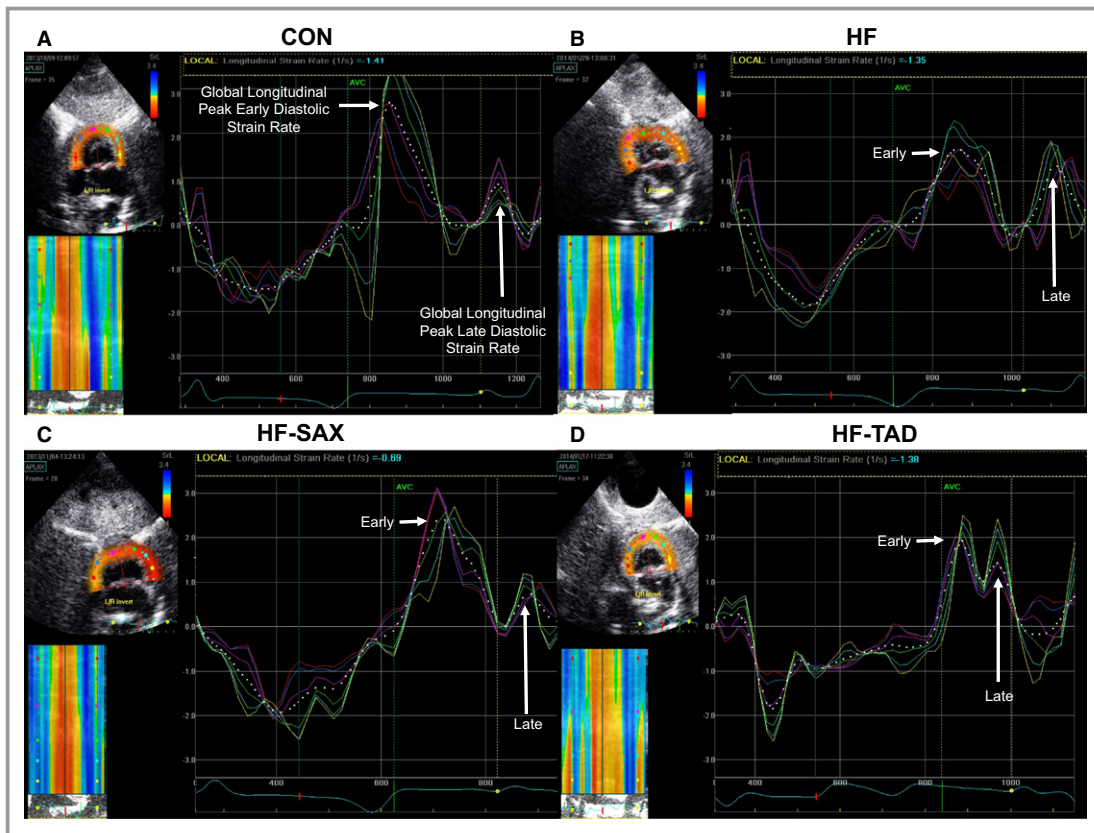


**Figure 6.** Left ventricular early and late diastolic mechanics. A through D, Representative 2DST echocardiography images from individual CON (A), HF (B), HF-SAX (C), and HF-TAD (D) animals highlighting a decrease in the early:late global longitudinal diastolic strain rate ratio in HF and HF-TAD animals compared to CON. This aortic banding–induced shift in LV diastolic mechanics, suggestive of diastolic dysfunction, was prevented in the HF-SAX group. E, Global longitudinal strain rate during early diastole was significantly reduced in the HF group, and to a greater extent in HF-TAD animals compared to CON. This effect of HF was attenuated in the HF-SAX group ( $*P<0.05$  vs CON,  $^{\dagger}P<0.05$  vs HF,  $^{\S}P<0.05$  vs HF-SAX). F, There was no effect of HF on apical circumferential early diastolic strain rate compared to CON animals. Mechanical movement in this plane was decreased in the HF-TAD group and increased in the HF-SAX group ( $*P<0.05$  vs CON,  $^{\dagger}P<0.05$  vs HF,  $^{\ddagger}P<0.05$  vs HF-TAD). G, LV early diastolic untwisting is increased in HF-SAX animals ( $*P<0.05$  vs all groups). H, LV global longitudinal late diastolic strain rate. Saxagliptin prevents increased global longitudinal late diastolic strain rate seen in the HF and HF-TAD groups ( $*P<0.05$  vs CON,  $^{\dagger}P<0.05$  vs HF-SAX). 2DST indicates 2-dimensional speckle tracking; CON, control; HF, heart failure; LV, left ventricular; SAX, saxagliptin; TAD, tadalafil.

showing sildenafil attenuated hypertrophy, decreased fibrosis, and restored LV relaxation kinetics in aortic-banded mice. Several preclinical and clinical studies followed investigating various methods of preserving cGMP levels, with beneficial results.<sup>5,9,10,15,44–46</sup> However, the sole multicenter study targeting this signaling in HFpEF, the RELAX trial (Effect of Phosphodiesterase-5 Inhibition on Exercise Capacity and Clinical Status in Heart Failure with Preserved Ejection Fraction), reported equivocal results after testing the PDE5 inhibitor sildenafil.<sup>47</sup> The results from our study did not completely reproduce the findings of Takimoto et al.<sup>6</sup> Although direct comparisons of the studies above are tempting, more importantly these differences provide a reminder that the translation of previous work in rodents to

larger mammals and/or humans is not inconsequential and should not be assumed.

### Limitations

Although the amino acid sequence of the BNP N-terminus in both humans and pigs is consistent with the substrate specificity of DPP-4, circulating levels of BNP are considerably lower in pigs compared to humans<sup>48</sup> and this feature of our model should be considered in interpreting our results. Our results showed plasma BNP and ANP levels were unchanged across groups, implying the beneficial effect of saxagliptin on fluid accumulation in the lungs was not dependent on unbalanced natriuretic peptide levels. However, our

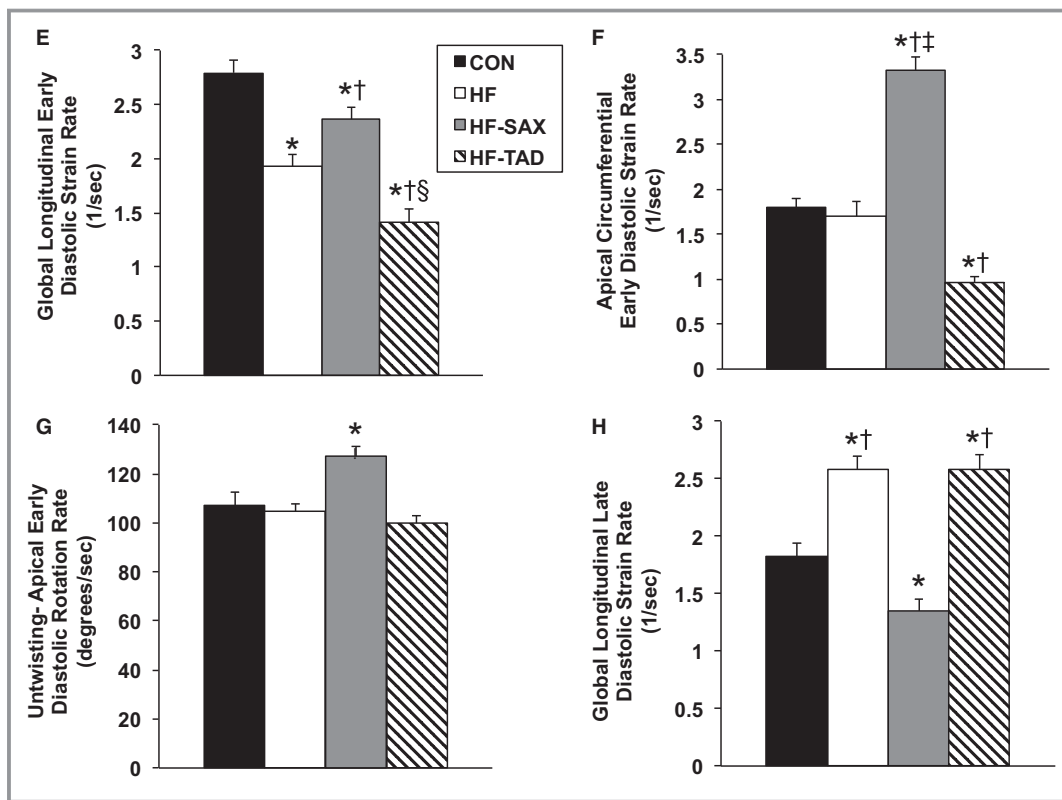


**Figure 6.** continued.

interpretation of these data is limited by methodology, as the radioimmunoassay used in the current study detects both BNP<sub>1-32</sub> and BNP<sub>3-32</sub> (or total BNP) and does not allow determination of the ratio of intact to cleaved BNP products. To the best of our knowledge, ours is the first study to demonstrate the beneficial effects of saxagliptin on a clinical characteristic of heart failure (lung congestion) in a large animal model of experimental HFpEF.

While both tadalafil and saxagliptin treatment altered the cGMP-PKG-PDE5 signaling axis, neither ultimately translated into an increase in PKG activity. Despite the doses of each drug being determined prior to the study using pharmacokinetic experiments to establish optimal oral administration equivalent to human standards, our findings could be interpreted to suggest the doses of each drug were suboptimal for the pig. Conversely, we could also reason that the saxagliptin dose was appropriate but given the demonstrated plasticity of PDE5 in our study, was ultimately ineffective in increasing net cGMP levels due to increased cGMP catabolism evident as increased PDE5 activity. Similarly, the 2.5-fold increase in cGMP expression in the HF-TAD group could be interpreted as evidence that our tadalafil dose was also appropriate. The lack of a subsequent increase in downstream PKG signaling in HF-TAD animals could be inferred as: (1) the observed increase in cGMP levels was

insufficient to stimulate downstream PKG activity; or (2) the activity of other phosphodiesterases such as PDE1 or PDE2 may have compensated for the inhibition of PDE5 by tadalafil. Indeed, both PDE1 and PDE2 have been shown to regulate the hydrolysis of cGMP.<sup>49</sup> Although outside the focus of the current study, our results suggest ideal therapeutic value could be gained from simultaneous administration of both drugs in parallel.

Our results also demonstrated that cGMP-PKG-PDE5 levels and activity were unchanged in the HF group, a finding not entirely inconsistent with human literature. The cGMP-PKG-PDE5 signaling axis has been hypothesized to contribute to the pathophysiology of human HF.<sup>6,50-52</sup> However, this finding is not definitive in a setting of human HFpEF<sup>5,9</sup> where clinical data have failed to show benefits previously reported in multiple animal models.<sup>47,50</sup> For example, van Heerebeek et al<sup>9</sup> found very low levels of cGMP and corresponding PKG activity in human HFpEF left ventricle that was not ascribed to PDE5 upregulation. Regardless, our findings imply that alterations to the cGMP-PKG-PDE5 signaling axis are not fundamental to the development or maintenance of HF in our animal model. Instead, our data suggest that the beneficial effects of saxagliptin on cardiac function may be mediated through reduced DPP-4 activity resulting in attenuation of circulating NPY levels.



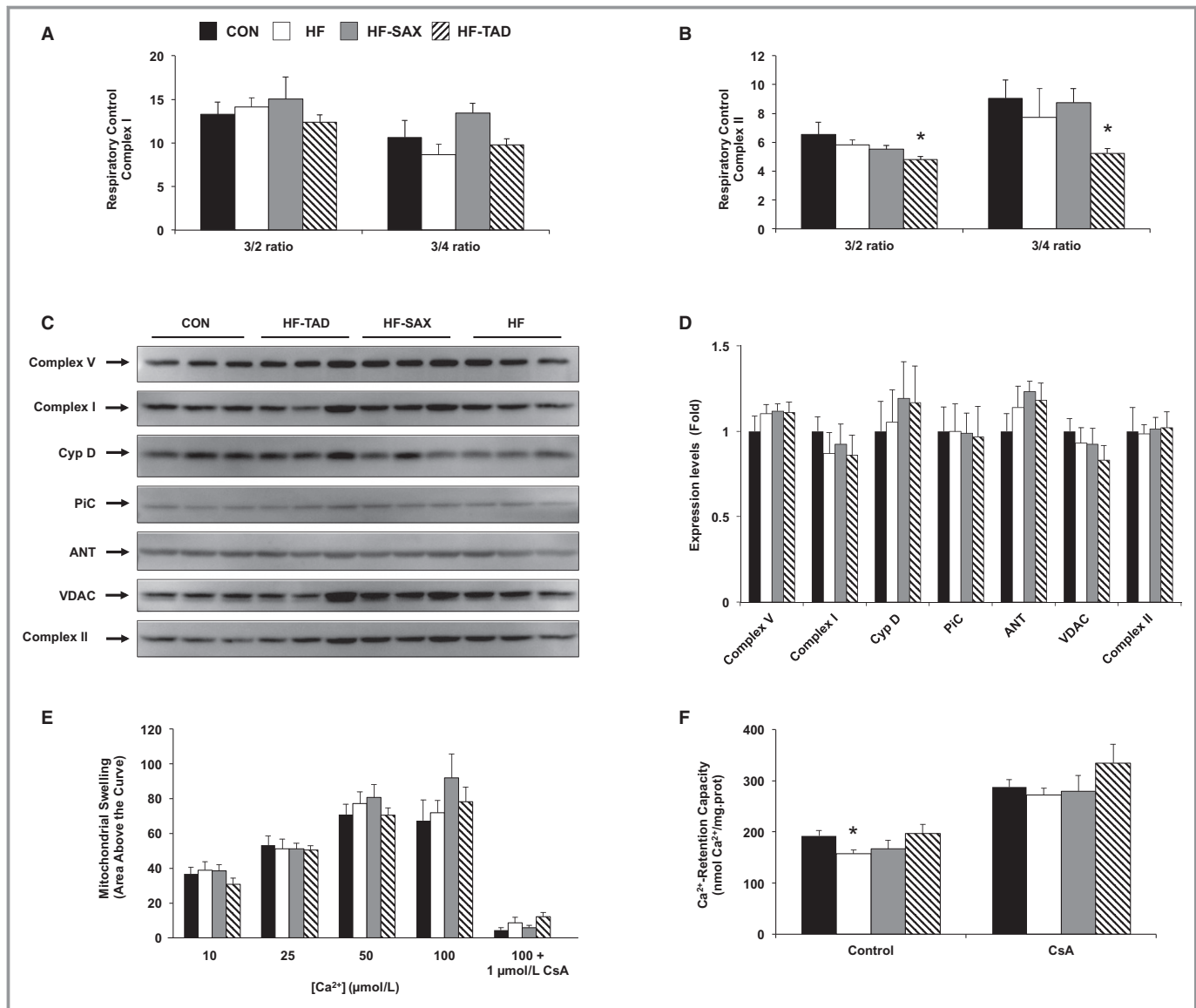


**Figure 7.** Comprehensive isolated mitochondrial function. A, Complex I-dependent respiratory control (R.C.) measured as the State3/State2 or State3/State4 ratio in isolated cardiac mitochondria was unchanged between groups. B, Complex II-dependent R.C. measured as the State3/State2 or State3/State4 ratio was decreased in HF-TAD animals compared to CON (\* $P < 0.05$  vs CON). C, Western blot analysis for respiratory chain and putative mitochondrial permeability transition (MPT) pore components ATP synthase (Complex V), NADH:ubiquinone oxidoreductase (Complex I), cyclophilin-D (CypD), mitochondrial phosphate carrier (PiC), adenine nucleotide translocase (ANT), voltage-dependent anion channel (VDAC) and succinate dehydrogenase (Complex II) in CON, HF, HF-SAX, and HF-TAD cardiac mitochondrial lysates. D, Quantification of the Western blot data ( $n = 6$  per group). E, Quantification of the area above the curve of the  $Ca^{2+}$ -induced swelling traces in isolated cardiac mitochondria was unchanged between groups (CsA, cyclosporine-A). F,  $Ca^{2+}$ -retention capacity was decreased in the HF group compared to CON (\* $P < 0.05$  vs CON), demonstrating increased susceptibility to  $Ca^{2+}$ -induced mitochondrial permeability transition (an early indicator of mitochondrial dysfunction). CON indicates control; HF, heart failure; SAX, saxagliptin; TAD, tadalafil.

## Conclusions

Chronic treatment with tadalafil and saxagliptin induced distinct changes in LV function and remodeling at both the organ and cellular level during the development of heart failure in a clinically relevant aortic-banded miniature swine model displaying key characteristics of HFpEF. Aortic banding

caused similar levels of concentric hypertrophy in all groups, although both saxagliptin and tadalafil prevented increased LV collagen deposition. Decreased fibrotic remodeling was correlated with the attenuation of increased NPY plasma levels. Each drug differentially altered the cGMP-PKG-PDE5 signaling axis, with tadalafil increasing myocardial cGMP levels and saxagliptin increasing PDE5 activity. However,

saxagliptin appears to be a superior candidate for the treatment of HFpEF when considering its comprehensive effects on integrated LV systolic and diastolic function.

## Acknowledgments

The authors would like to thank Dr David Kass, Melissa Cobb, Dr Thomas Reilly, Dr Charles Wiedmeyer, Anne Gibson, and Emily Dehn for their considerable technical contributions and consultation, which were essential for the completion of the study. We would also like to thank Gore for their generous gift of vascular Gore-Tex sleeves used in our aortic-banding procedures.

## Disclosures

This study was supported with funding from AstraZeneca (C.A. Emter).

## References

- Borlaug BA, Paulus WJ. Heart failure with preserved ejection fraction: pathophysiology, diagnosis, and treatment. *Eur Heart J*. 2011;32:670–679.
- Maeder MT, Kaye DM. Heart failure with normal left ventricular ejection fraction. *J Am Coll Cardiol*. 2009;53:905–918.
- Oktay AA, Rich JD, Shah SJ. The emerging epidemic of heart failure with preserved ejection fraction. *Curr Heart Fail Rep*. 2013;10:401–410.
- Sharma K, Kass DA. Heart failure with preserved ejection fraction: mechanisms, clinical features, and therapies. *Circ Res*. 2014;115:79–96.
- Greene SJ, Gheorghiane M, Borlaug BA, Pieske B, Vaduganathan M, Burnett JC Jr, Roessig L, Stasch JP, Solomon SD, Paulus WJ, Butler J. The cGMP signaling pathway as a therapeutic target in heart failure with preserved ejection fraction. *J Am Heart Assoc*. 2013;2:e000536.
- Takimoto E, Champion HC, Li M, Belardi D, Ren S, Rodriguez ER, Bedja D, Gabrielson KL, Wang Y, Kass DA. Chronic inhibition of cyclic GMP phosphodiesterase 5A prevents and reverses cardiac hypertrophy. *Nat Med*. 2005;11:214–222.
- Borbely A, Falcao-Pires I, van Heerebeek L, Hamdani N, Edes I, Gavina C, Leite-Moreira AF, Bronzwaer JG, Papp Z, van der Velden J, Stienen GJ, Paulus WJ. Hypophosphorylation of the stiff N2B titin isoform raises cardiomyocyte resting tension in failing human myocardium. *Circ Res*. 2009;104:780–786.
- Kruger M, Kotter S, Grutzner A, Lang P, Andresen C, Redfield MM, Butt E, dos Remedios CG, Linke WA. Protein kinase G modulates human myocardial passive stiffness by phosphorylation of the titin springs. *Circ Res*. 2009;104:87–94.
- van Heerebeek L, Hamdani N, Falcao-Pires I, Leite-Moreira AF, Begieneman MP, Bronzwaer JG, van der Velden J, Stienen GJ, Laarman GJ, Somsen A, Verheugt FW, Niessen HW, Paulus WJ. Low myocardial protein kinase G activity in heart failure with preserved ejection fraction. *Circulation*. 2012;126:830–839.
- Tsai EJ, Kass DA. Cyclic GMP signaling in cardiovascular pathophysiology and therapeutics. *Pharmacol Ther*. 2009;122:216–238.
- dos Santos L, Salles TA, Arruda-Junior DF, Campos LC, Pereira AC, Barreto AL, Antonio EL, Mansur AJ, Tucci PJ, Krieger JE, Girardi AC. Circulating dipeptidyl peptidase IV activity correlates with cardiac dysfunction in human and experimental heart failure. *Circ Heart Fail*. 2013;6:1029–1038.
- Brandt I, Lambeir AM, Ketelslegers JM, Vanderheyden M, Scharpe S, De Meester I. Dipeptidyl-peptidase IV converts intact B-type natriuretic peptide into its des-SerPro form. *Clin Chem*. 2006;52:82–87.
- Boerrigter G, Costello-Boerrigter LC, Harty GJ, Lapp H, Burnett JC Jr. Deserine-proline brain natriuretic peptide 3-32 in cardiorenal regulation. *Am J Physiol Regul Integr Comp Physiol*. 2007;292:R897–R901.
- Scheen AJ. Cardiovascular effects of gliptins. *Nat Rev Cardiol*. 2013;10:73–84.
- Solomon SD, Zile M, Pieske B, Voors A, Shah A, Kraigher-Krainer E, Shi V, Bransford T, Takeuchi M, Gong J, Lefkowitz M, Packer M, McMurray JJ. Prospective comparison of AwarBoMOhfwpefl. The angiotensin receptor neprilysin inhibitor LCZ696 in heart failure with preserved ejection fraction: a phase 2 double-blind randomised controlled trial. *Lancet*. 2012;380:1387–1395.
- Hiemstra JA, Gutierrez-Aguilar M, Marshall KD, McCommis KS, Zgoda PJ, Cruz-Rivera N, Jenkins NT, Krenz M, Domeier TL, Baines CP, Emter CA. A new twist on an old idea part 2: cyclosporine preserves normal mitochondrial but not cardiomyocyte function in mini-swine with compensated heart failure. *Physiol Rep*. 2014;2:e12050.
- Hiemstra JA, Liu S, Ahlman MA, Schuleri KH, Lardo AC, Baines CP, Dellsperger KC, Bluemke DA, Emter CA. A new twist on an old idea: a two-dimensional speckle tracking assessment of cyclosporine as a therapeutic alternative for heart failure with preserved ejection fraction. *Physiol Rep*. 2013;1:e00174.
- Marshall KD, Muller BN, Krenz M, Hanft LM, McDonald KS, Dellsperger KC, Emter CA. Heart failure with preserved ejection fraction: chronic low-intensity interval exercise training preserves myocardial O<sub>2</sub> balance and diastolic function. *J Appl Physiol*. 2013;114:131–147.
- Emter CA, Baines CP. Low-intensity aerobic interval training attenuates pathological left ventricular remodeling and mitochondrial dysfunction in aortic-banded miniature swine. *Am J Physiol Heart Circ Physiol*. 2010;299:H1348–H1356.
- Wrishko R, Sorsaburu S, Wong D, Strawbridge A, McGill J. Safety, efficacy, and pharmacokinetic overview of low-dose daily administration of tadalafil. *J Sex Med*. 2009;6:2039–2048.
- Mondillo S, Galderisi M, Mele D, Cameli M, Lomoriello VS, Zaca V, Ballo P, D'Andrea A, Muraru D, Losi M, Agricola E, D'Errico A, Buralli S, Sciomer S, Nistri S, Badano L; Echocardiography Study Group Of The Italian Society Of C. Speckle-tracking echocardiography: a new technique for assessing myocardial function. *J Ultrasound Med*. 2011;30:71–83.
- Russel IK, Gotte MJ, Bronzwaer JG, Knaapen P, Paulus WJ, van Rossum AC. Left ventricular torsion: an expanding role in the analysis of myocardial dysfunction. *JACC Cardiovasc Imaging*. 2009;2:648–655.
- McDonald KS, Hanft LM, Domeier TL, Emter CA. Length and PKA dependence of force generation and loaded shortening in porcine cardiac myocytes. *Biochem Res Int*. 2012;2012:371415.
- Lee DI, Zhu G, Sasaki T, Cho GS, Hamdani N, Holewinski R, Jo SH, Danner T, Zhang M, Rainer PP, Bedja D, Kirk JA, Ranek MJ, Dostmann WR, Kwon C, Margulies KB, Van Eyk JE, Paulus WJ, Takimoto E, Kass DA. Phosphodiesterase 9A controls nitric-oxide-independent cGMP and hypertrophic heart disease. *Nature*. 2015;519:472–476.
- Burnett JC Jr, Kao PC, Hu DC, Hesser DW, Heublein D, Granger JP, Oppenorth TJ, Reeder GS. Atrial natriuretic peptide elevation in congestive heart failure in the human. *Science*. 1986;231:1145–1147.
- Seilhamer JJ, Arfsten A, Miller JA, Lundquist P, Scarborough RM, Lewicki JA, Porter JG. Human and canine gene homologs of porcine brain natriuretic peptide. *Biochem Biophys Res Commun*. 1989;165:650–658.
- Sudoh T, Maekawa K, Kojima M, Minamino N, Kangawa K, Matsuo H. Cloning and sequence analysis of cDNA encoding a precursor for human brain natriuretic peptide. *Biochem Biophys Res Commun*. 1989;159:1427–1434.
- Pieske B, Kretschmann B, Meyer M, Holubarsch C, Weirich J, Posival H, Minami K, Just H, Hasenfuss G. Alterations in intracellular calcium handling associated with the inverse force-frequency relation in human dilated cardiomyopathy. *Circulation*. 1995;92:1169–1178.
- Sabatini S, Sgro P, Duranti G, Ceci R, Di Luigi L. Tadalafil alters energy metabolism in C2C12 skeletal muscle cells. *Acta Biochim Pol*. 2011;58:237–241.
- Ishikawa K, Agüero J, Oh JG, Hammoudi N, Fish LA, Leonardson L, Picatoste B, Santos-Gallego CG, Fish KM, Hajjar RJ. Increased stiffness is the major early abnormality in a pig model of severe aortic stenosis and predisposes to congestive heart failure in the absence of systolic dysfunction. *J Am Heart Assoc*. 2015;4:e001925.
- Yarbrough WM, Mukherjee R, Stroud RE, Rivers WT, Oelsen JM, Dixon JA, Eckhouse SR, Ikonomidis JS, Zile MR, Spinale FG. Progressive induction of left ventricular pressure overload in a large animal model elicits myocardial remodeling and a unique matrix signature. *J Thorac Cardiovasc Surg*. 2012;143:215–223.
- Ye Y, Gong G, Ochiai K, Liu J, Zhang J. High-energy phosphate metabolism and creatine kinase in failing hearts: a new porcine model. *Circulation*. 2001;103:1570–1576.
- Szardien S, Mollmann H, Voss S, Troidl C, Rolf A, Liebetrau C, Rixe J, Elsasser A, Hamm CW, Nef HM. Elevated serum levels of neuropeptide Y in stress cardiomyopathy. *Int J Cardiol*. 2011;147:155–157.
- Dvorakova MC, Kruzliak P, Rabkin SW. Role of neuropeptides in cardiomyopathies. *Peptides*. 2014;61:1–6.
- Shanks J, Herring N. Peripheral cardiac sympathetic hyperactivity in cardiovascular disease: role of neuropeptides. *Am J Physiol Regul Integr Comp Physiol*. 2013;305:R1411–R1420.
- Zoccali C, Mallamaci F, Tripepi G, Benedetto FA, Parlongo S, Cutrupi S, Bonanno G, Rapisarda F, Fatuzzo P, Seminara G, Cataliotti A, Malatino LS.

- Neuropeptide Y, left ventricular mass and function in patients with end stage renal disease. *J Hypertens*. 2003;21:1355–1362.
37. Santos-Gallego CG, Vahl TP, Goliasch G, Picatoste B, Arias T, Ishikawa K, Njerve IU, Sanz J, Narula J, Sengupta P, Hajjar RJ, Fuster V, Badimon JJ. The sphingosine 1-phosphate receptor agonist fingolimod increases myocardial salvage and decreases adverse post-infarction left ventricular remodeling in a porcine model of ischemia-reperfusion. *Circulation*. 2016;133:954–966.
  38. Zhang R, Niu H, Kang X, Ban T, Hong H, Ai J. Long-term administration of neuropeptide Y in the subcutaneous infusion results in cardiac dysfunction and hypertrophy in rats. *Cell Physiol Biochem*. 2015;37:94–104.
  39. Anamthakmakula P, Sahu M, Sahu A. Evidence suggesting phosphodiesterase-3B regulation of NPY/AgRP gene expression in mHypoE-46 hypothalamic neurons. *Neurosci Lett*. 2015;604:113–118.
  40. Morris DA, Boldt LH, Eichstadt H, Ozcelik C, Haverkamp W. Myocardial systolic and diastolic performance derived by 2-dimensional speckle tracking echocardiography in heart failure with normal left ventricular ejection fraction. *Circ Heart Fail*. 2012;5:610–620.
  41. Carlsson M, Ugander M, Heiberg E, Arheden H. The quantitative relationship between longitudinal and radial function in left, right, and total heart pumping in humans. *Am J Physiol Heart Circ Physiol*. 2007;293:H636–H644.
  42. Pavlopoulos H, Nihoyannopoulos P. Abnormal segmental relaxation patterns in hypertensive disease and symptomatic diastolic dysfunction detected by strain echocardiography. *J Am Soc Echocardiogr*. 2008;21:899–906.
  43. Schiattarella GG, Hill JA. Inhibition of hypertrophy is a good therapeutic strategy in ventricular pressure overload. *Circulation*. 2015;131:1435–1447.
  44. Hoffmann LS, Chen HH. cGMP: transition from bench to bedside: a report of the 6th international conference on cGMP generators, effectors and therapeutic implications. *Naunyn Schmiedeberg Arch Pharmacol*. 2014;387:707–718.
  45. Guazzi M, Vicenzi M, Arena R, Guazzi MD. Pulmonary hypertension in heart failure with preserved ejection fraction: a target of phosphodiesterase-5 inhibition in a 1-year study. *Circulation*. 2011;124:164–174.
  46. Moens AL, Takimoto E, Tocchetti CG, Chakir K, Bedja D, Cormaci G, Ketner EA, Majmudar M, Gabrielson K, Halushka MK, Mitchell JB, Biswal S, Channon KM, Wolin MS, Alp NJ, Paolucci N, Champion HC, Kass DA. Reversal of cardiac hypertrophy and fibrosis from pressure overload by tetrahydrobiopterin: efficacy of recoupling nitric oxide synthase as a therapeutic strategy. *Circulation*. 2008;117:2626–2636.
  47. Redfield MM, Chen HH, Borlaug BA, Semigran MJ, Lee KL, Lewis G, LeWinter MM, Rouleau JL, Bull DA, Mann DL, Deswal A, Stevenson LW, Givertz MM, Ofili EO, O'Connor CM, Felker GM, Goldsmith SR, Bart BA, McNulty SE, Ibarra JC, Lin G, Oh JK, Patel MR, Kim RJ, Tracy RP, Velazquez EJ, Anstrom KJ, Hernandez AF, Mascette AM, Braunwald E, Trial R. Effect of phosphodiesterase-5 inhibition on exercise capacity and clinical status in heart failure with preserved ejection fraction: a randomized clinical trial. *JAMA*. 2013;309:1268–1277.
  48. Aburaya M, Minamino N, Kangawa K, Tanaka K, Matsuo H. Distribution and molecular forms of brain natriuretic peptide in porcine heart and blood. *Biochem Biophys Res Commun*. 1989;165:872–879.
  49. Lee DI, Kass DA. Phosphodiesterases and cyclic GMP regulation in heart muscle. *Physiology (Bethesda)*. 2012;27:248–258.
  50. Zhang M, Kass DA. Phosphodiesterases and cardiac cGMP: evolving roles and controversies. *Trends Pharmacol Sci*. 2011;32:360–365.
  51. Pokreisz P, Vandenwijngaert S, Bito V, Van den Bergh A, Lenaerts I, Busch C, Marsboom G, Gheysens O, Vermeersch P, Biesmans L, Liu X, Gillijns H, Pellens M, Van Lommel A, Buys E, Schoonjans L, Vanhaecke J, Verbeken E, Sipido K, Herijgers P, Bloch KD, Janssens SP. Ventricular phosphodiesterase-5 expression is increased in patients with advanced heart failure and contributes to adverse ventricular remodeling after myocardial infarction in mice. *Circulation*. 2009;119:408–416.
  52. Nagendran J, Archer SL, Soliman D, Gurtu V, Moudgil R, Haromy A, St Aubin C, Webster L, Rebecka IM, Ross DB, Light PE, Dyck JR, Michelakis ED. Phosphodiesterase type 5 is highly expressed in the hypertrophied human right ventricle, and acute inhibition of phosphodiesterase type 5 improves contractility. *Circulation*. 2007;116:238–248.